AD 463370

THE ANTENNA LABORATORY

RESEARCH ACTIVITIES in ---

Automatic Controls | *Antennas* | *Echo Area Studies*
Microwave Circuits | *Astronautics* | *E M Field Theory*
Terrain Investigations | *Radomes* | *Systems Analysis*
Wave Propagation | | *Submillimeter Applications*

FAR-FIELD PATTERN PREDICTION
FOR SHIPBOARD ANTENNAS

Gary A. Thiele

Contract No. N123(953)-31663A

1522-11 March 31 1965

Prepared for:
United States Navy Electronics Laboratory
Code 3300b
San Diego, California

Department of ELECTRICAL ENGINEERING

THE OHIO STATE UNIVERSITY
RESEARCH FOUNDATION
Columbus, Ohio

REPORT 1522-11

REPORT
by
THE OHIO STATE UNIVERSITY RESEARCH FOUNDATION
COLUMBUS, OHIO 43212

Sponsor	United States Navy Electronics Laboratory San Diego, California
Contract	N123(953)-31663A
Investigation of	Study Program Related to Shipboard Antenna System Environment
Subject of Report	Far-Field Pattern Prediction for Shipboard Antennas
Submitted by	Gary A. Thiele Antenna Laboratory Department of Electrical Engineering
Date	31 March 1965

ABSTRACT

Shipboard antennas operate in the vicinity of the ship's superstructure which consists of numerous metallic scatterers of various sizes and shapes. The far-field patterns of shipboard antennas are perturbed by these scatterers and are therefore difficult to predict. In this report a method is discussed for approximating the far-field pattern in the horizontal plane of a thin vertical antenna (e.g., a whip antenna) near cylindrical scatterers of arbitrary cross-section whose physical heights are at least that of the antenna. The method is based on approximating the antenna with an infinite line source and the scatterer with an array of thin infinite wires.

Some representative calculated and experimental results are presented which generally show very good agreement between the predicted and measured patterns. In addition, limitations of the method are discussed and the computer programs for calculating the far-field patterns are explained in some detail.

TABLE OF CONTENTS

FAR-FIELD PATTERN PREDICTION FOR SHIPBOARD ANTENNAS

I. INTRODUCTION

Radiation from shipboard antennas is complicated by the presence of the many varied objects that make up the ship's superstructure. This environment influences the far-field pattern of an antenna as well as its terminal impedance and can affect the mutual coupling between any two antennas. This report will be concerned only with the first problem, namely the effect of the superstructure on the far-field pattern in the horizontal plane of a thin vertical radiator, which is a good approximation for most MF and many HF antennas.

The technique used to predict the perturbed far-field pattern is essentially an extension of Richmond's [1] method for predicting the scattering pattern of an arbitrary array of infinitely long, thin, parallel wires. He has shown that a solid cylindrical conducting object can be approximated, for the purpose of pattern calculation, by replacing the object with thin parallel wires located at its periphery, if there are at least five wires per wavelength and one wire defines each corner. For a given form of the incident wave (e.g., plane waves, or cylindrical waves which will be used in this report) complex currents are induced on each of the wires. These induced currents are then assumed to radiate into free space to form a scattering pattern which can be calculated by the far-field radiation integral.

Essentially the same procedure is followed here, and a line source parallel to the wire array is used to approximate a thin vertical antenna as shown in Fig. 1. A computer program then gives the far-field pattern of the line source plus the field scattered by the wires, that is, the approximate pattern of the antenna in the presence of the scatterer.

The question naturally arises whether or not a technique which employs infinitely long wires and an infinitely long line source with uniform current can predict with acceptable accuracy the far-field of a finite antenna with a non-uniform current in the presence of a conducting cylinder of finite height. The answer is "yes" within certain restrictions. Justification for this positive answer was obtained experimentally; the correspondence between the predicted and measured patterns was generally quite good.

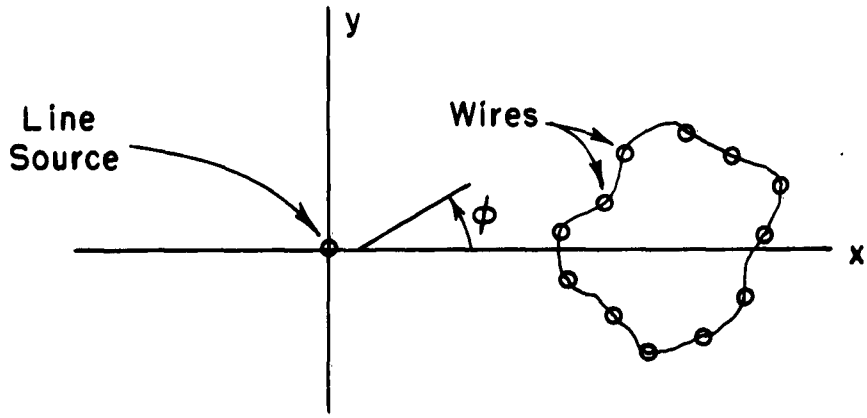

Fig. 1. Mathematical model for the case of a line source radiating in the presence of a cylindrical structure.

II. RESULTS

A. General

The results of this research consist of (1) a group of computer programs to calculate the patterns of the antenna (represented by a line source) and the cylindrical scatterers (represented by wire arrays), and (2) an extensive set of measurements to establish the range of validity of the calculations.

The mathematical formulation of the problem is given in Appendix A. The equations in this appendix are the equations on which the computer programs are based. The computer programs for use with a moderate-size (IBM 1620) computer are given and explained in Appendix B. Three passes through the computer are required; the output of the first pass is obtained on IBM cards and is used as the input to the second pass, and the output of this pass is similarly used as input for the third, which yields the desired results. A sample calculation is given in Appendix C to illustrate the use of these programs. The computer programs for use with a large (IBM 7094) computer are given in Appendix D. During the project it turned out efficient to use the smaller computer for initial investigations but the larger for "production" runs. The "production" program is being optimized further to allow the generation of a handbook of patterns with a reasonable use of computer time.

The experimental program was designed to test the calculations. Two types of approximations are involved in the calculations, and the

experimental program was designed to test these independently. One approximation consists of replacing finite antennas and obstacles with infinite ones to simplify the computations. To test this approximation, the models (described in more detail below) consisted of antennas and obstacles between two parallel plates, of which one could be removed. With the top plate in place, the patterns should be the same as for the infinite structure used in the calculations, except for finite groundplane effects. With the top plate removed, the structure approximates the practical finite case. Comparison of the two patterns shows the effect of the approximation. The second approximation involves replacing the solid scatterer with an array of wires and the numerical approximations of the programs. The errors involved here are estimated by the differences between the measured patterns with both plates in place and the calculated patterns. Finally, the overall accuracy can be evaluated by comparing the computed patterns with the measured patterns with the top plate removed.

B. Experimental Model

The model used for the measurements is shown in Figs. 2 and 3. At 2 Gc the structure is approximately 5 wavelengths in diameter, excluding the one-wavelength long flare. The feed is off center, being 2λ from the nearest portion of the flare. The styrofoam dielectric ring is one-half wavelength thick and slightly less than one-half wavelength tall. The height of the ring was chosen so that the plate spacing would be less than $\lambda/2$. In order to obtain an omnidirectional pattern with the top plate in place and no obstacle present it was necessary to adjust the top of the exciting probe so that it terminated about $\frac{1}{16}$" from the top plate. With the top plate on an experimental check was possible of the infinite case itself, whereas with the top plate absent the more practical finite case could be measured and checked against the patterns predicted and measured for the infinite case.

C. Comparison of Measurements and Calculations

Several solid metallic scattering objects were tested with the parallel-plate structure. These included circular cylinders with diameters from $\lambda/4$ to λ and square cylinders whose sides were either $\lambda/4$ or $\lambda/2$. Patterns were measured and calculated for various distances between source and obstacle using these scatterers. In all cases good agreement between the measured and calculated patterns was obtained. Some representative results are discussed in the following paragraphs.

Figure 4 shows a cylinder of square cross-section positioned a distance d from a vertical source and Fig. 5 a,b,c,d show the associated

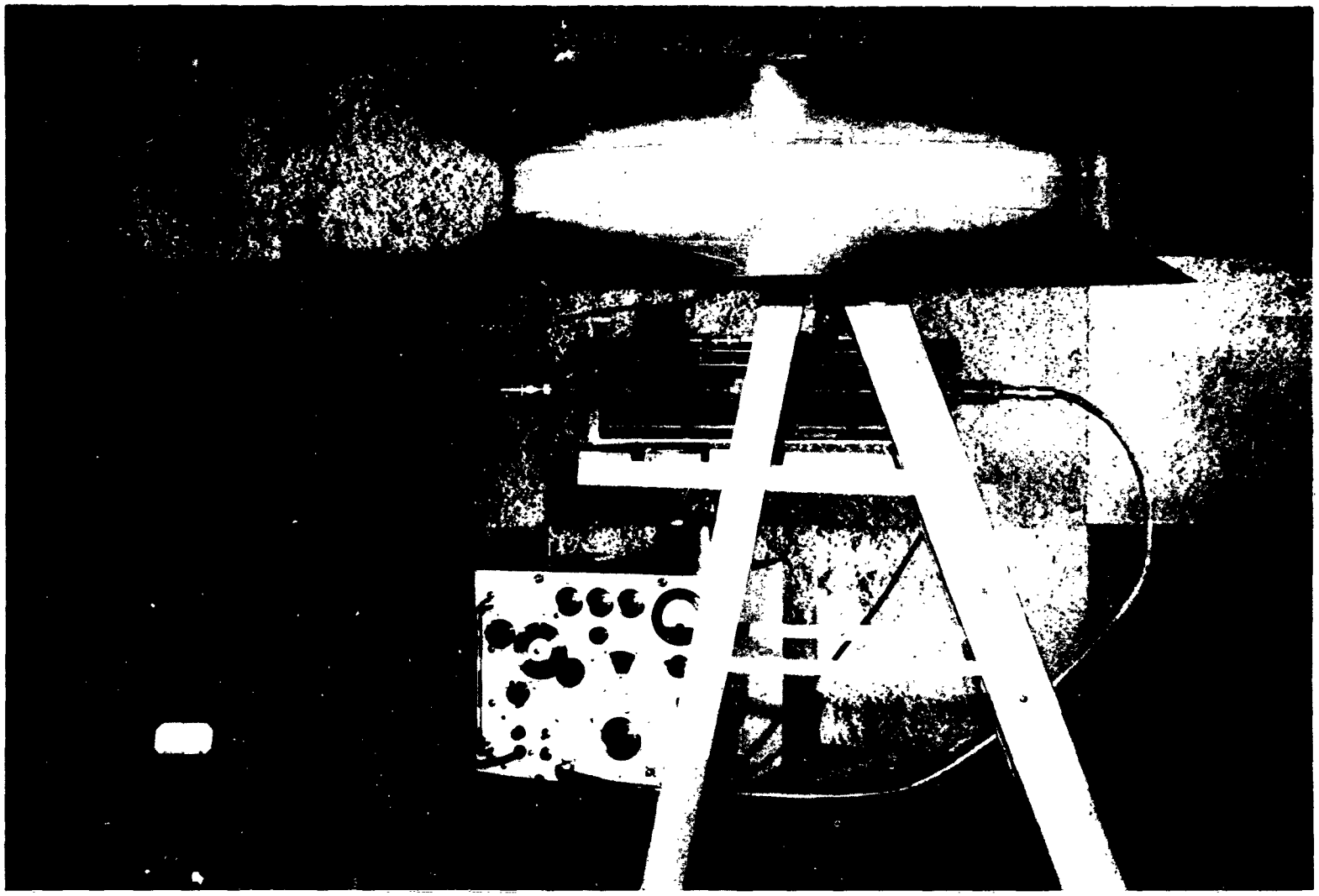

Fig. 2. Parallel-plate device as it would appear on an outdoor pattern range.

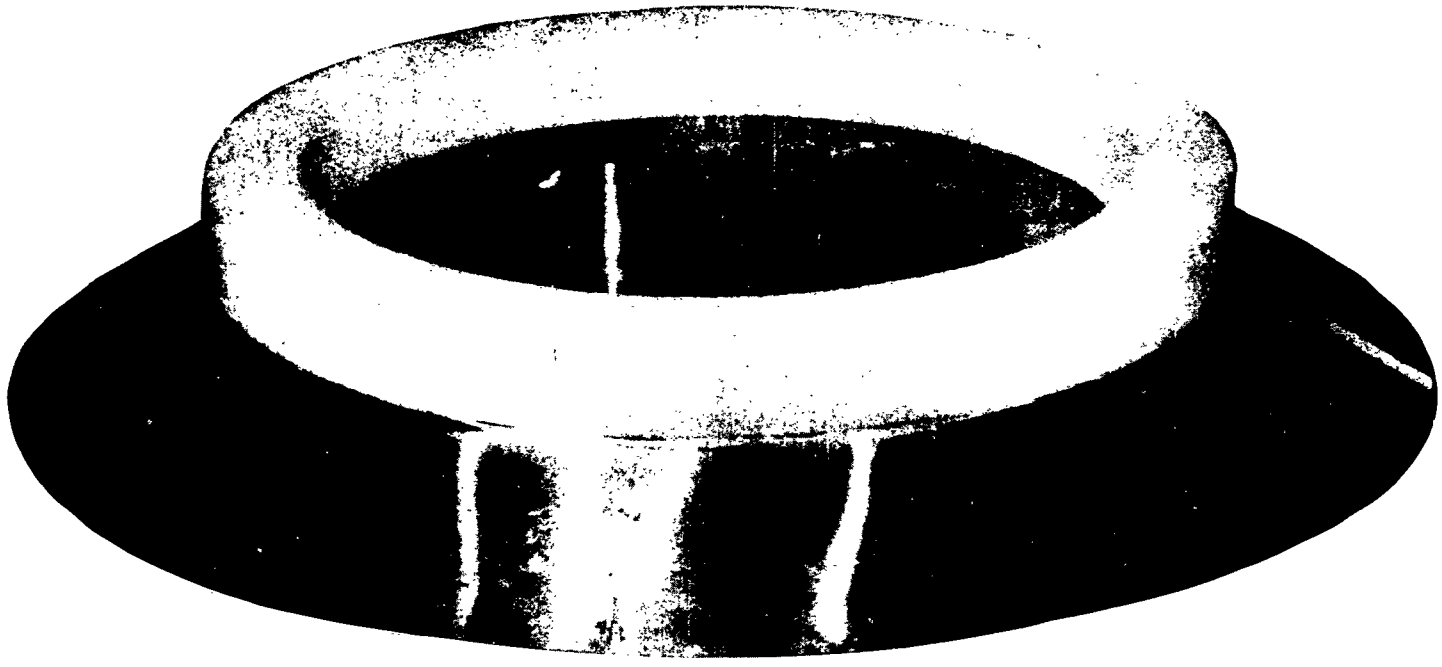

Fig. 3. Parallel-plate structure with top plate removed.

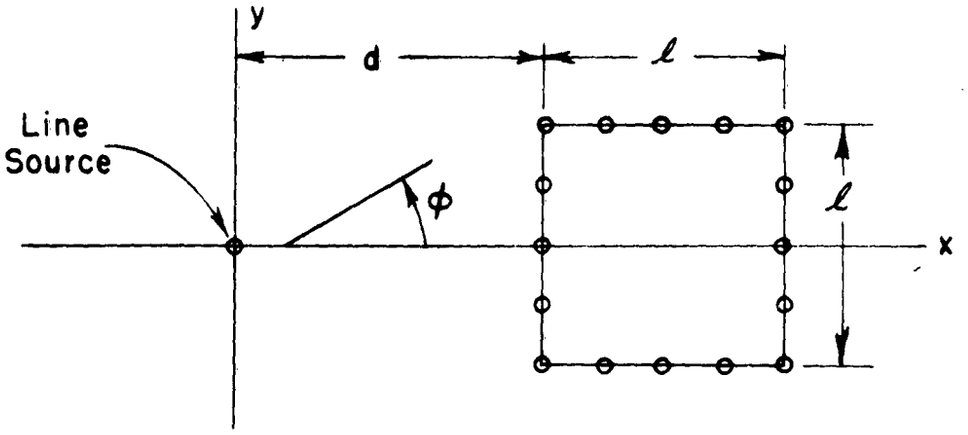

Fig. 4. Square cylinder near a line source.

far-field patterns for various values of d with $\ell = \lambda/4$. The omnidirectional patterns shown as a reference for the calculated patterns correspond to the antenna without scattering obstacles. It can be seen that in general the measured patterns change little when the top plate is removed and also that the theoretical patterns are in good agreement with the experimental ones, especially for the smaller values of d. The reason for the small lobe in the forward scatter direction with the top-plate absent will be explained shortly. The theoretical pattern was determined by representing the cylinder by 5 wires on a side. Equally good results can be obtained with as few as three wires, that is, a wire at each corner and one in between. The effect of the number of wires on the calculated pattern is shown in Fig. 6. Because of symmetry only that part of the pattern between zero degrees and 180 degrees is shown. Essentially the same pattern is obtained using either 5 or 3 wires per side. If only 4 wires total (i.e., one at each corner) are used, the pattern deteriorates appreciably. On the other hand using 8 wires on a side (i.e., a density of 32 wires per wavelength) causes a slight shift in the pattern opposite to that when there were only 4 wires total. Also, increasing the wire density at the corners has negligible effect. Consequently, nothing is gained by using an excessive wire density and valuable storage space in the computer is wasted, a fact that may be of considerable importance in cases where large and/or numerous scatterers are present. In addition, the number of wires necessary to represent an object may be reduced by carefully eliminating those wires on the forward scatter side of the scatterer as shown in Fig. 7. The corresponding far-field pattern functions for the three cases of Fig. 7 are shown in Fig. 8. The pattern for the case where no wires are omitted is almost identically

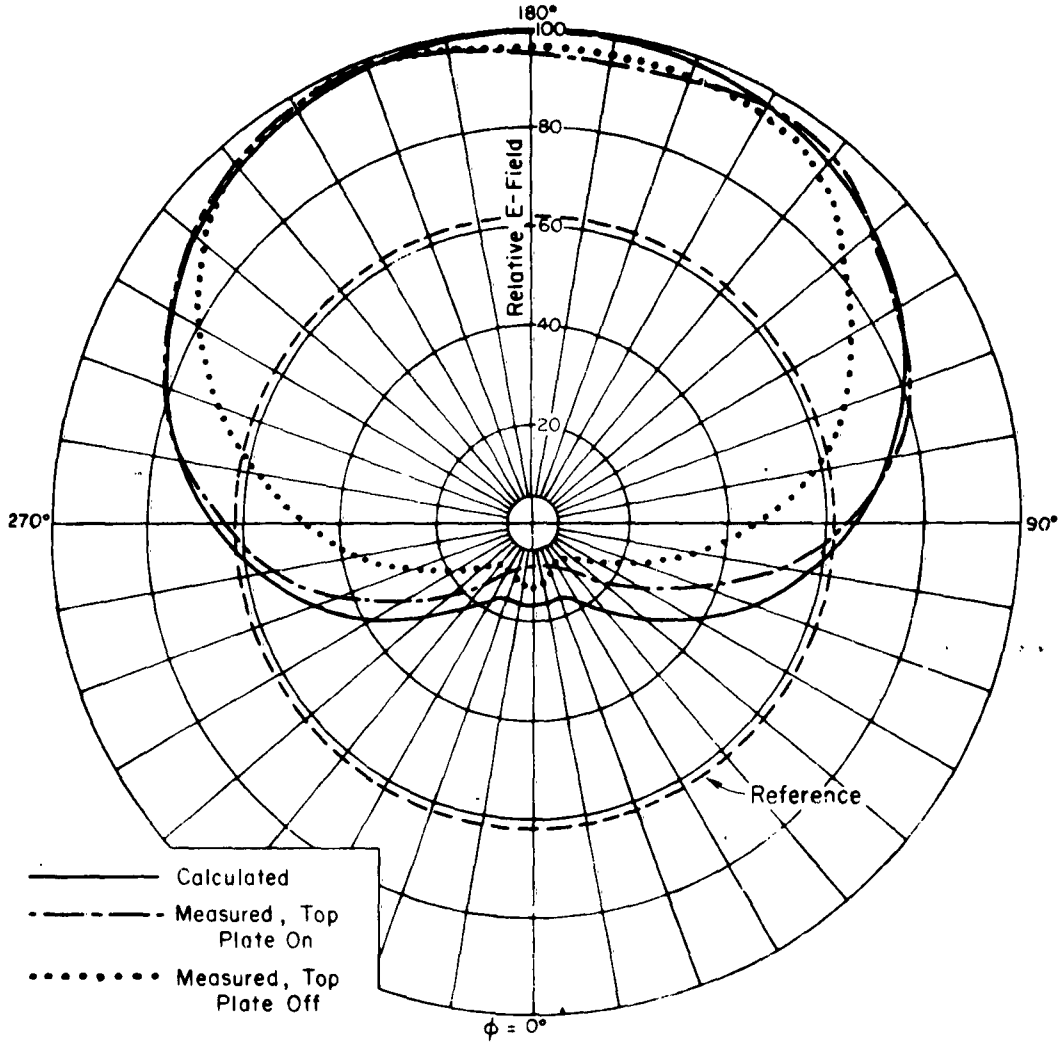

Fig. 5a. Far-field patterns of a square cylinder, $\ell = \lambda/4$.
(a) $d = \lambda/4$.

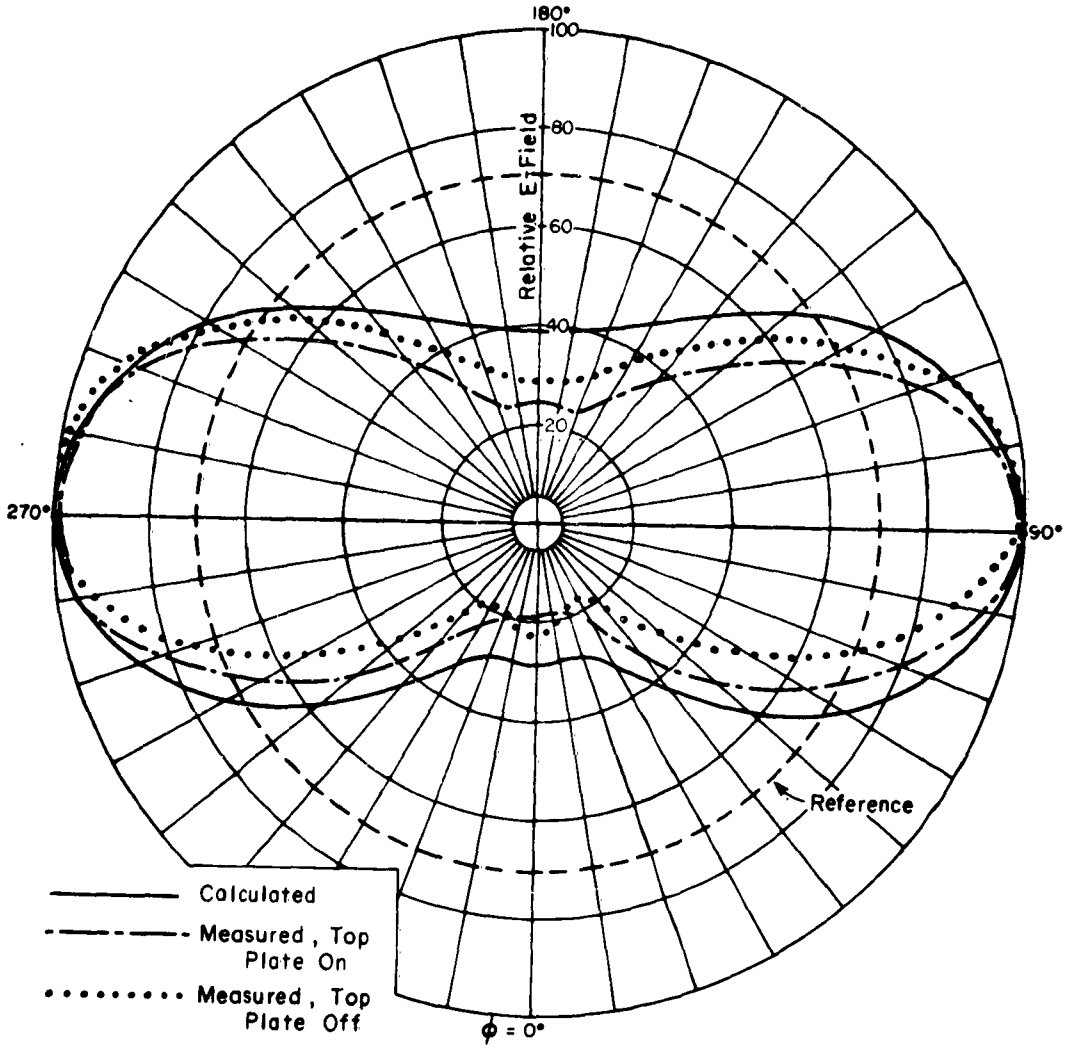

Fig. 5b. Far-field patterns of a square cylinder, $\ell = \lambda/4$.
(b) $d = \lambda/2$.

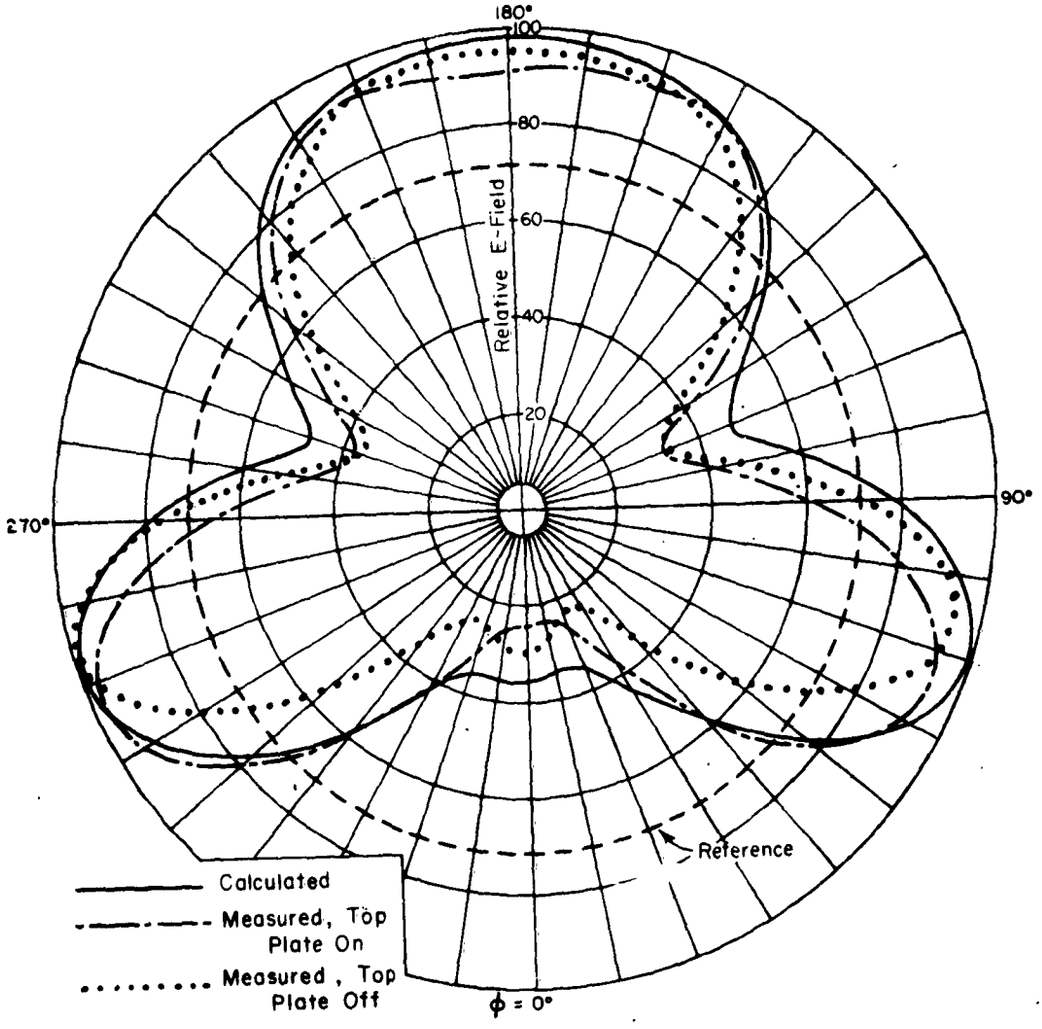

Fig. 5c. Far-field patterns of a square cylinder, $\ell = \lambda/4$.
(c) $d = 3\lambda/4$.

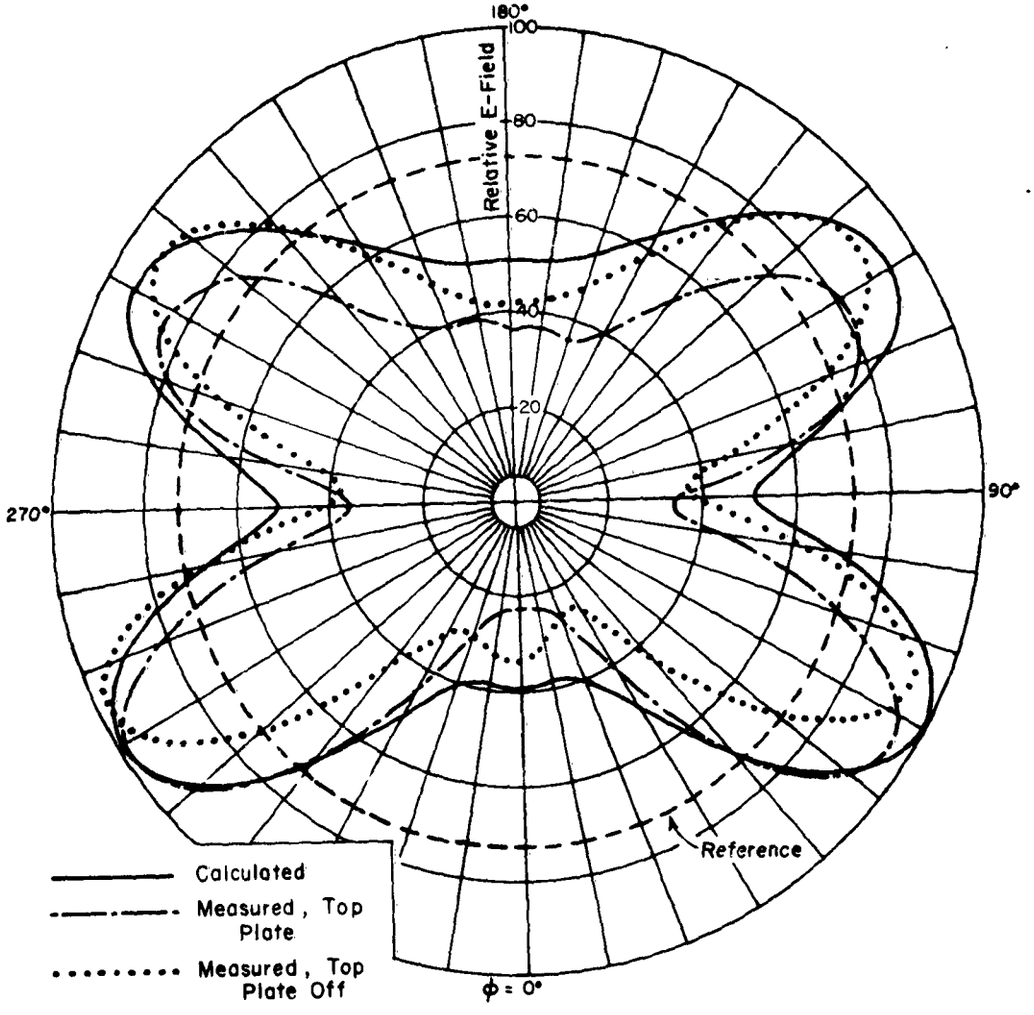

Fig. 5d. Far-field patterns of a square cylinder, $\ell = \lambda/4$.
(d) $d = \lambda$.

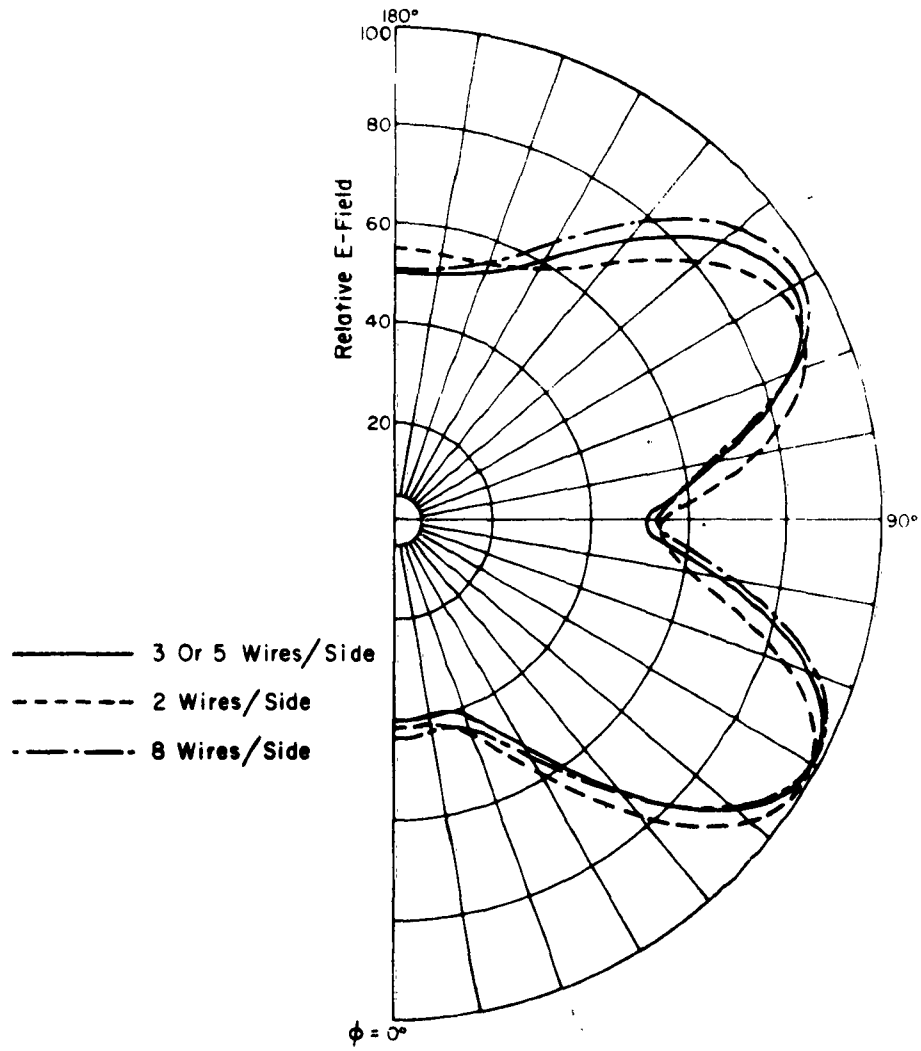

Fig. 6 Effect of the number of wires on the calculated pattern, $d = \lambda$, $\ell = \lambda/4$.

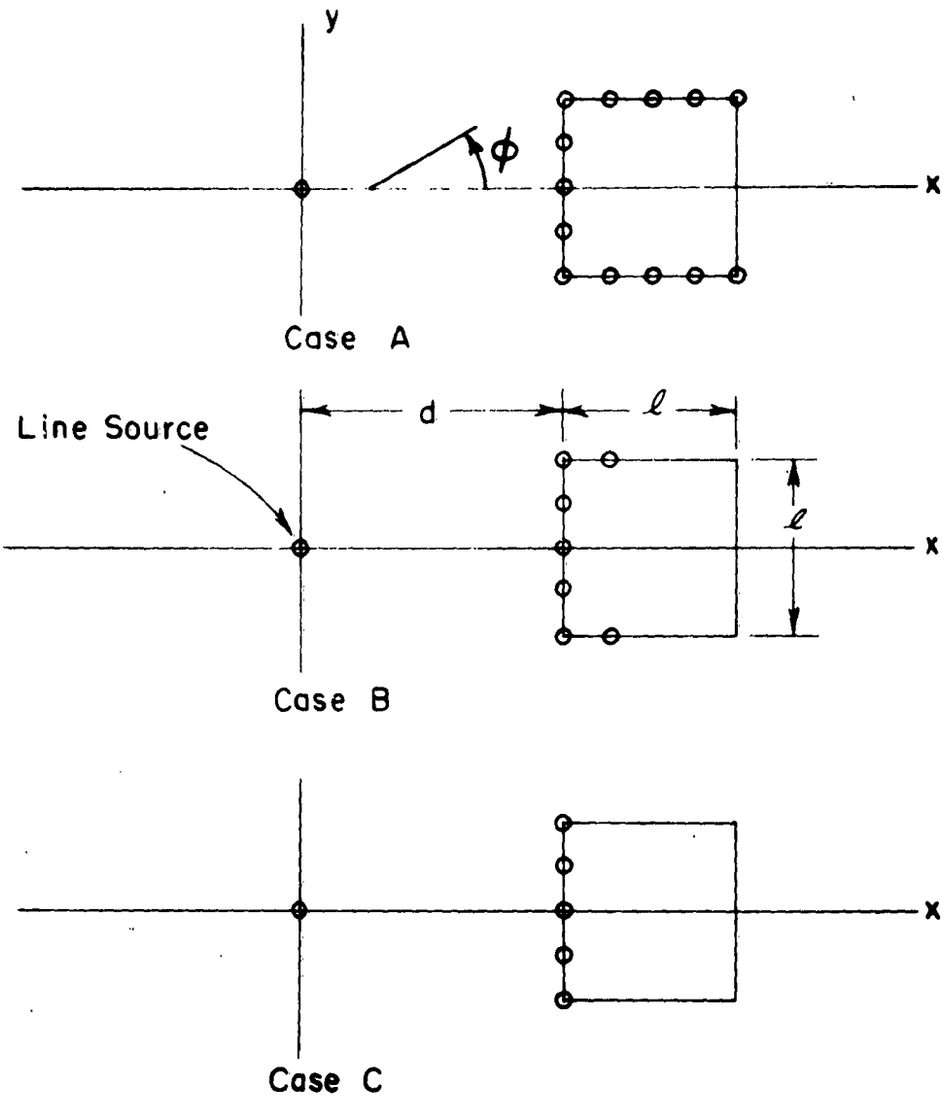

Fig. 7. Wires omitted on the forward-scatter side of a square cylinder.

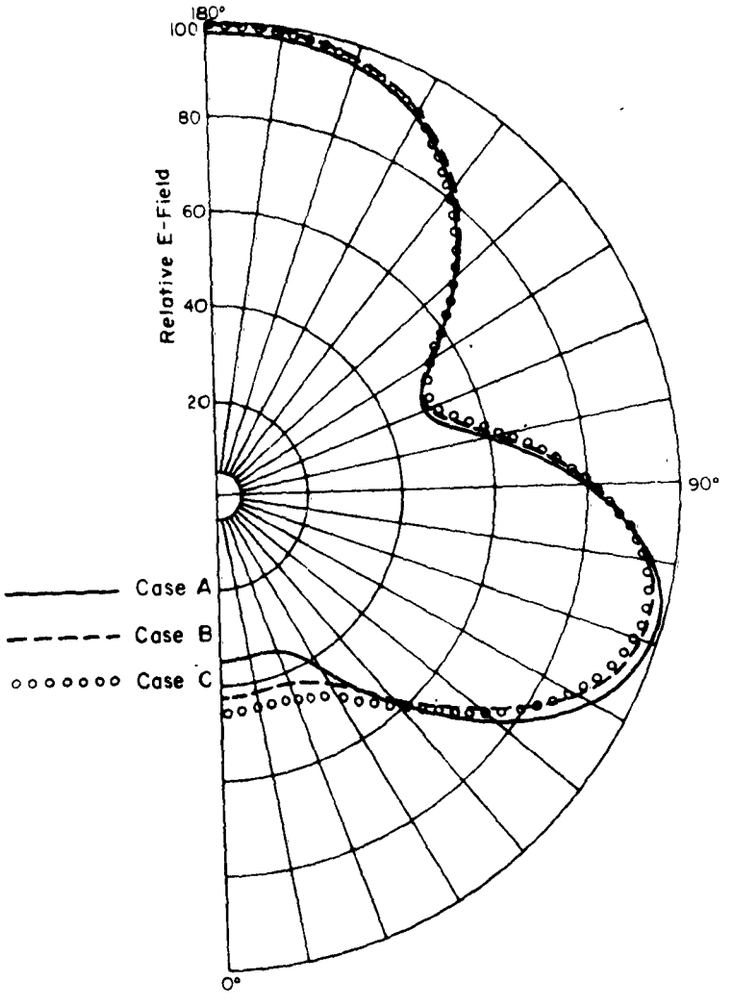

Fig. 8. Patterns for the configurations in Fig. 7.

equal to pattern A while patterns B and C show differences mostly in the forward scatter direction. The reason some of the wires may be eliminated without seriously affecting the pattern is that the currents of those wires on the forward side are quite small compared to those on the back, and therefore they contribute insignificantly to the far-field pattern. When the square cylinder is rotated 45° about its center, it was found that almost half of the wires could be eliminated without seriously changing the pattern. This situation is illustrated in Fig. 9.

Several sets of patterns were taken for the square cylinder $\lambda/2$ on a side as shown in Fig. 9 except that calculations were made with wires on all four sides. Again agreement between experimental and theoretical patterns was good as shown in Figs. 10 a, b, c, d. It is interesting to note that the patterns in Fig. 10 and Fig. 5 are not too dissimilar for corresponding values of d even though the size and orientation of the scatterer are not the same. This fact is further supported by the case of a circular cylinder near a line source, as illustrated in Fig. 11. Figure 12 shows the predicted patterns for d equal to $\lambda/2$ and λ for cylinders whose diameters are $\lambda/2$ and λ. Thus it is seen that source-to-scatterer distance is the most sensitive parameter and that in general, for small objects, the size and shape of the scatterer are important but to a lesser degree.

The experimental patterns in Figs. 5 and 10 were recorded with the height of the source approximately equal to that of the scatterer; these patterns exhibit a small minor lobe in the forward-scatter direction that is neither predicted by theory nor measured when the top plate is in place.

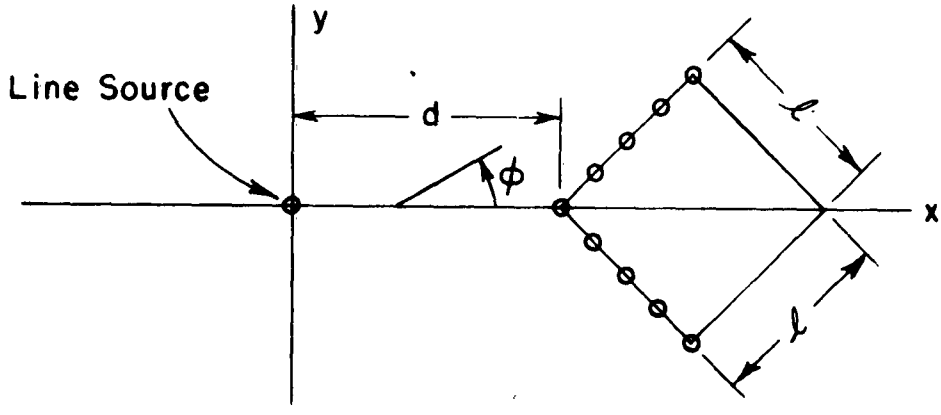

Fig. 9. Wires omitted on the forward-scatter side of a square cylinder rotated 45°.

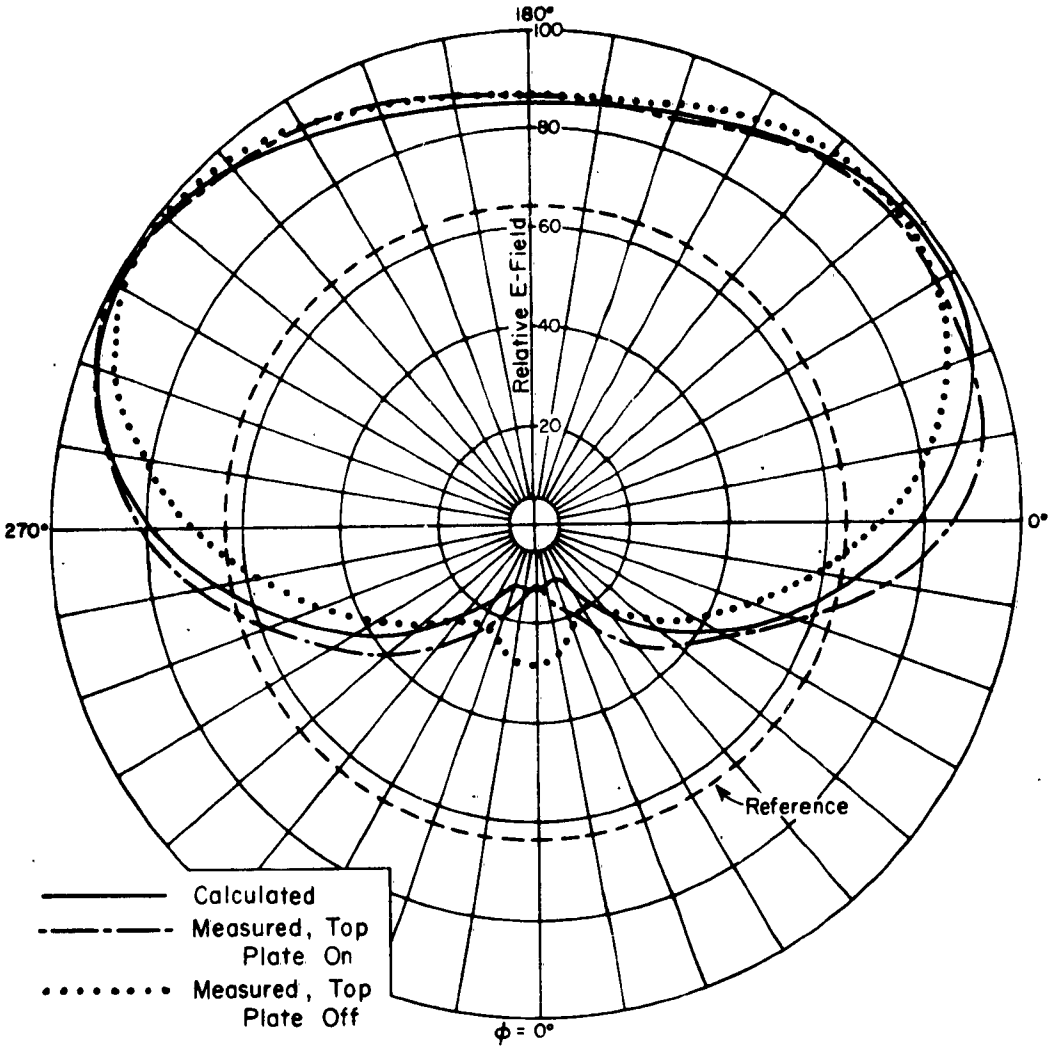

Fig. 10a. Far-field patterns of a square cylinder rotated 45°.
(a) $d = \lambda/4$.

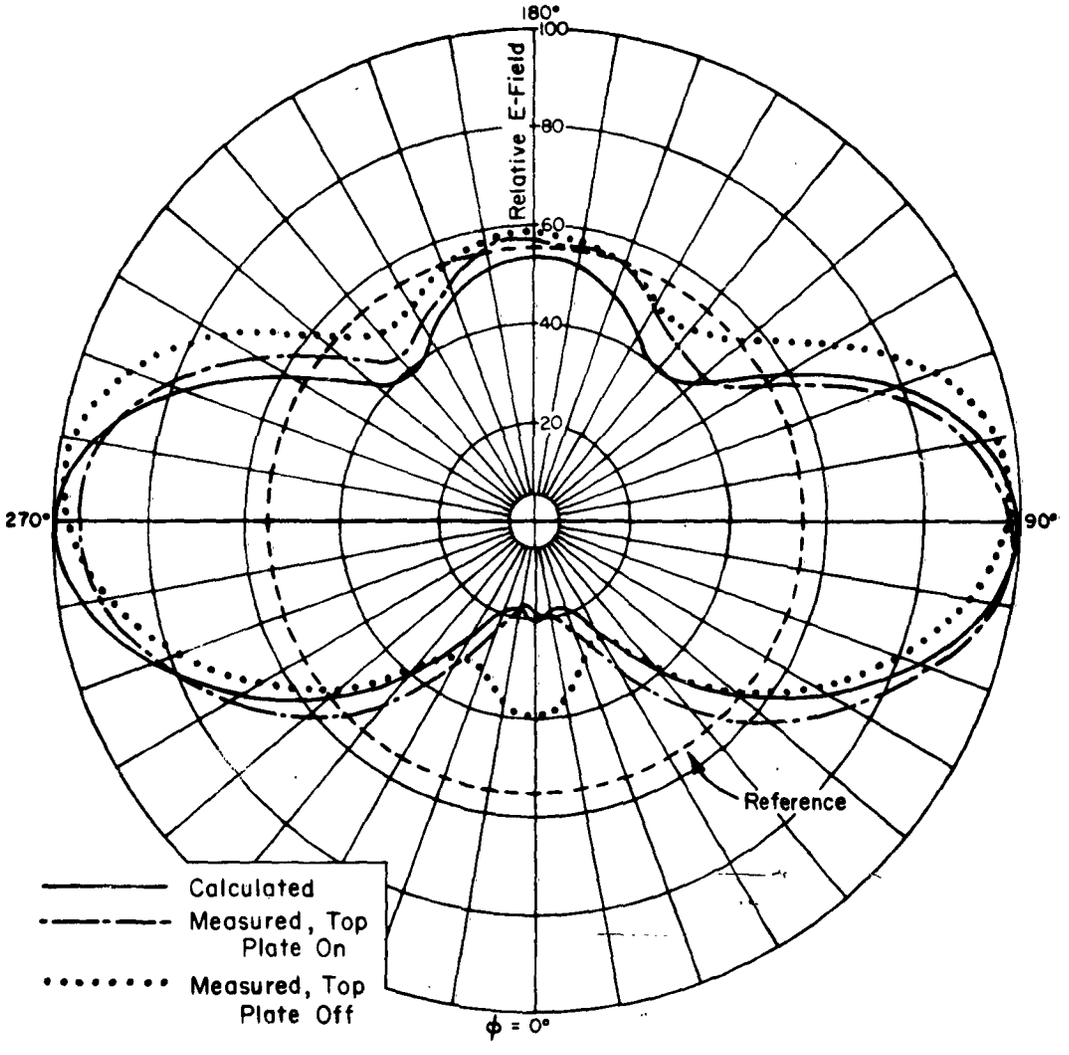

Fig. 10b. Far-field patterns of a square cylinder rotated 45°.
(b) $d = \lambda/2$.

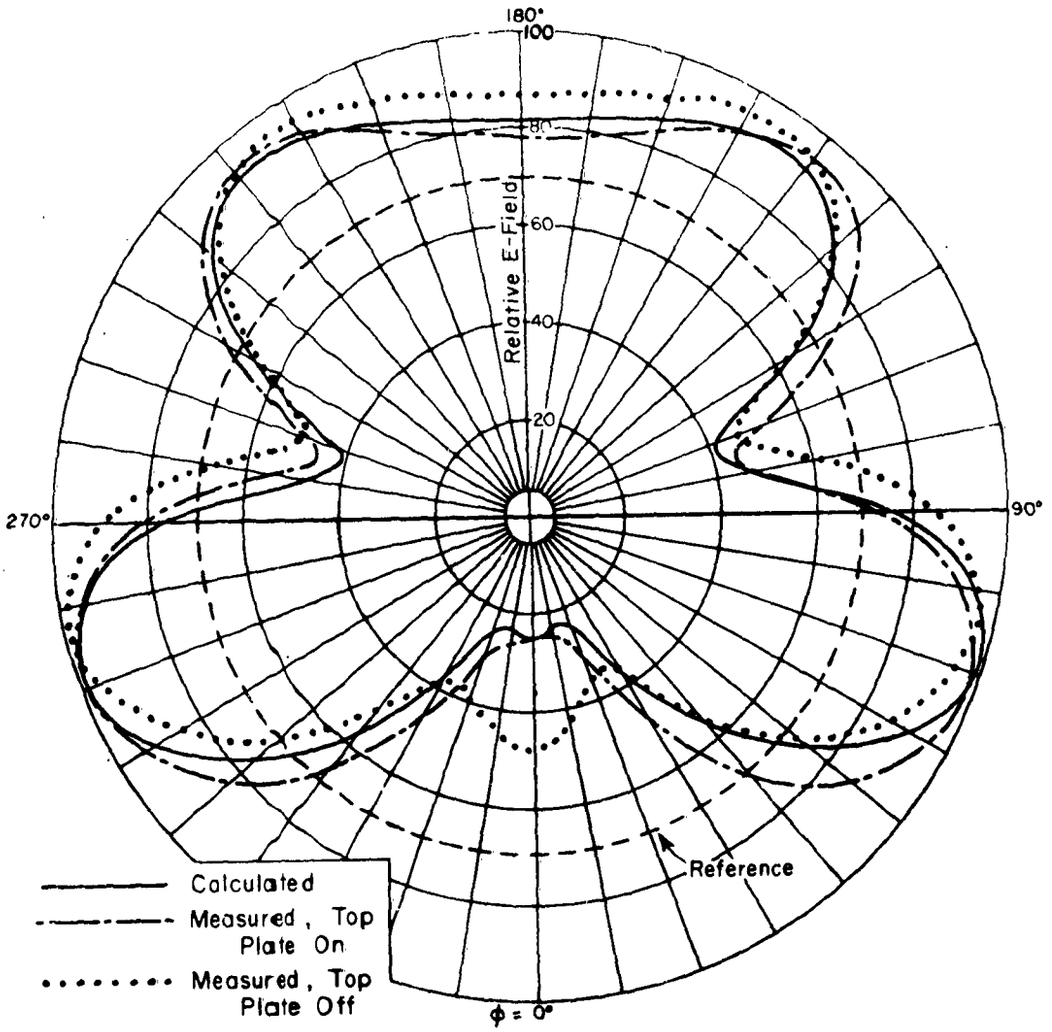

Fig. 10c. Far-field patterns of a square cylinder rotated 45°.
(c) $d = 3\lambda/4$.

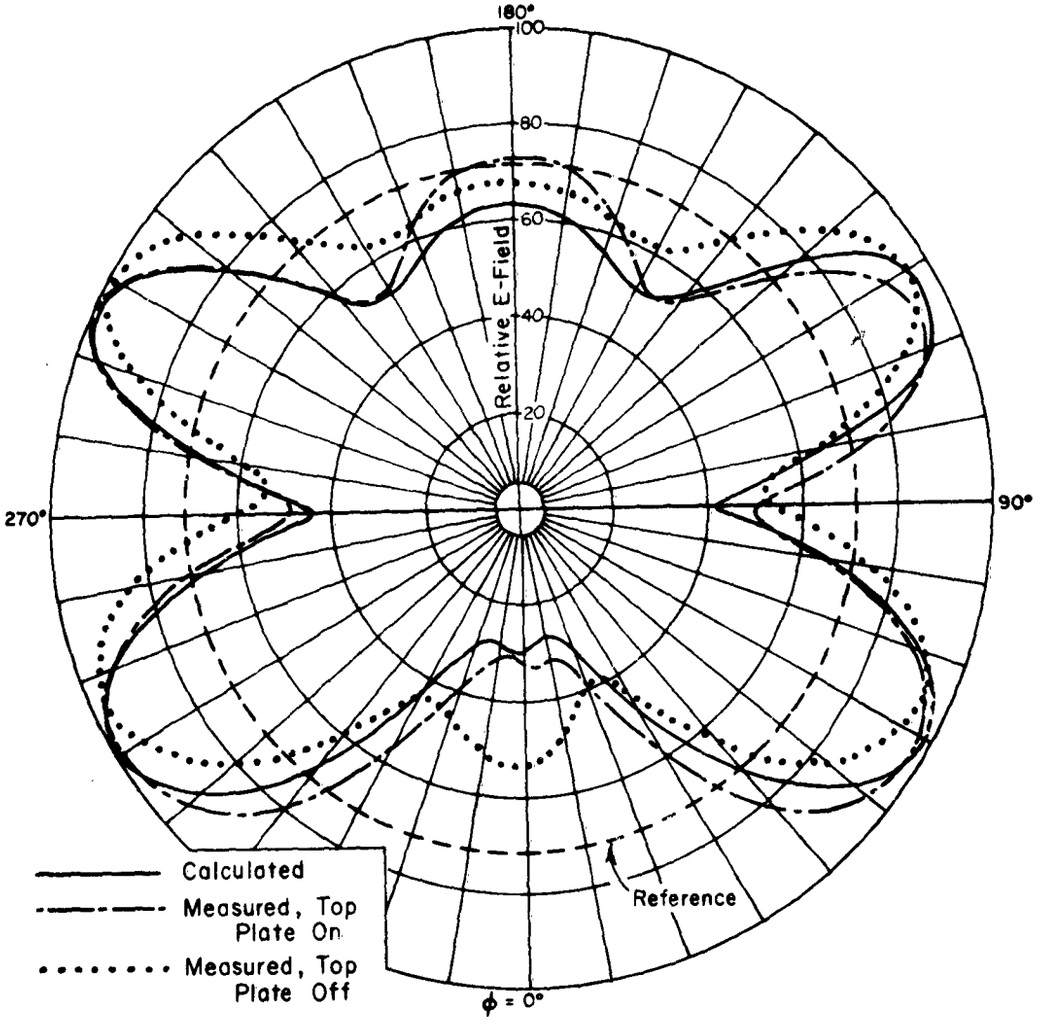

Fig. 10d. Far-field patterns of a square cylinder rotated 45°.
(d) $d = \lambda$.

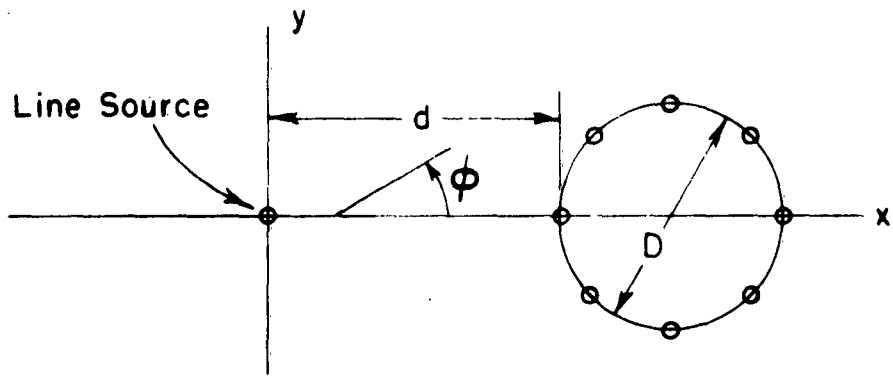

Fig. 11. Circular cylinder near a line source.

The existence of this minor lobe is explained by Fig. 13. The orientation of the scatterer is the same as that in Fig. 9 with $\ell = \lambda/4$, $d = \lambda/4$ and the variable being the cylinder height h. The source antenna height h_s was just under $\lambda/2$ and the experimental scatterer was a solid cylinder. It is apparent from Fig. 13 that the small lobe in Figs. 5 and 10 is caused by diffraction over the top of the cylinder and that this does not take place if the cylinder height is on the order of twice that of the source. Also, for the case where the source is taller than the scatterer considerable energy is propagated over the top. Consequently, the method of far-field pattern prediction described in this report can not be expected to give very accurate results for situations where the antenna is taller than the scatterer. However, some insight into the shape of the pattern in back-scatter direction may be obtained depending on how much smaller the scatterer is than the source antenna.

III. CONCLUSIONS

It has been shown that the far-field pattern in the horizontal plane of a vertical antenna near cylindrical scattering objects of finite height can be predicted with reasonable accuracy by representing the scatterer by an array of infinitely-long parallel wires and the vertical antenna by an infinitely-long line source. The far-field predictions are valid so long as the scatterer is at least as tall as the antenna itself and at least 5 wires per wavelength are used to represent the object. The additional restriction is made that the number of wires used must sufficiently define the shape of the scatterer. Also, in situations where computer

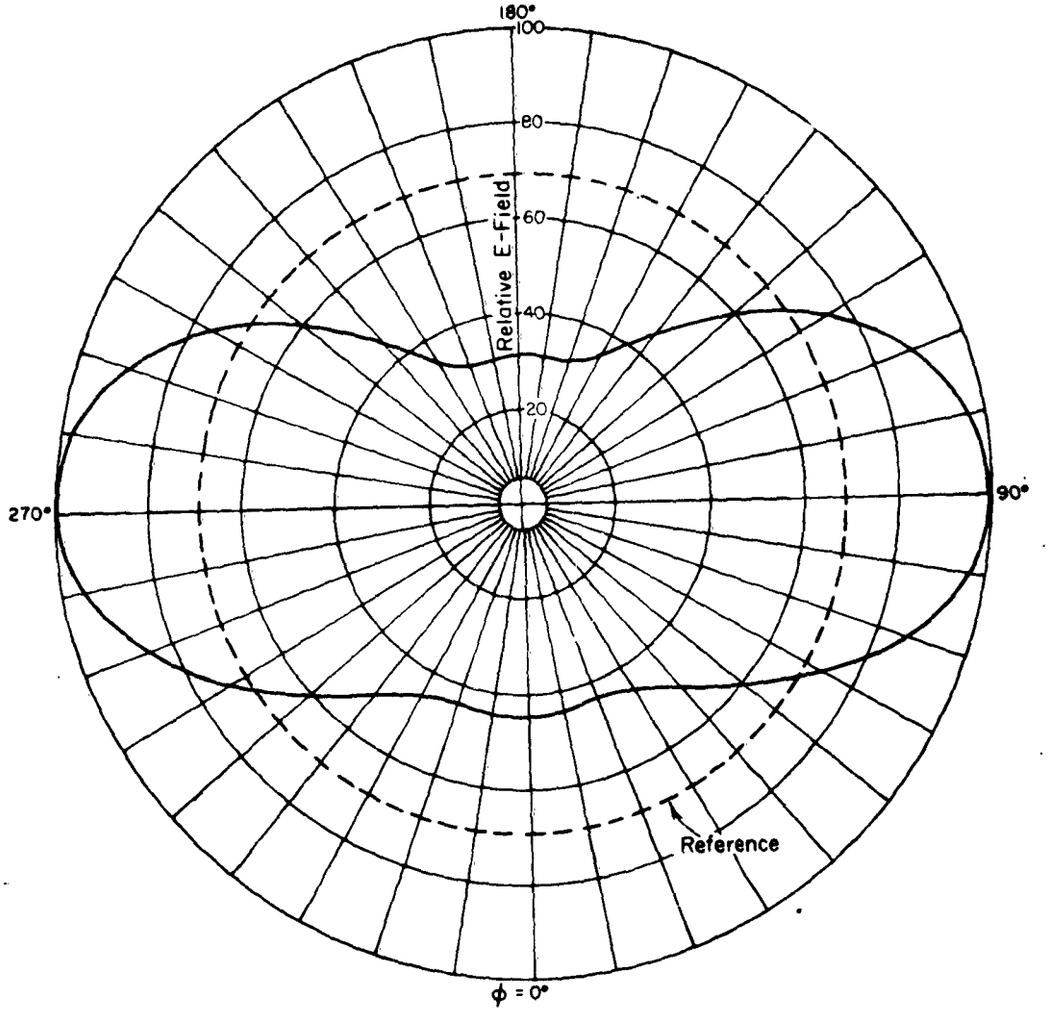

Fig. 12a. Theoretical far-field patterns of a circular cylinder.
(a) $d = \lambda/2$, $D = \lambda/4$.

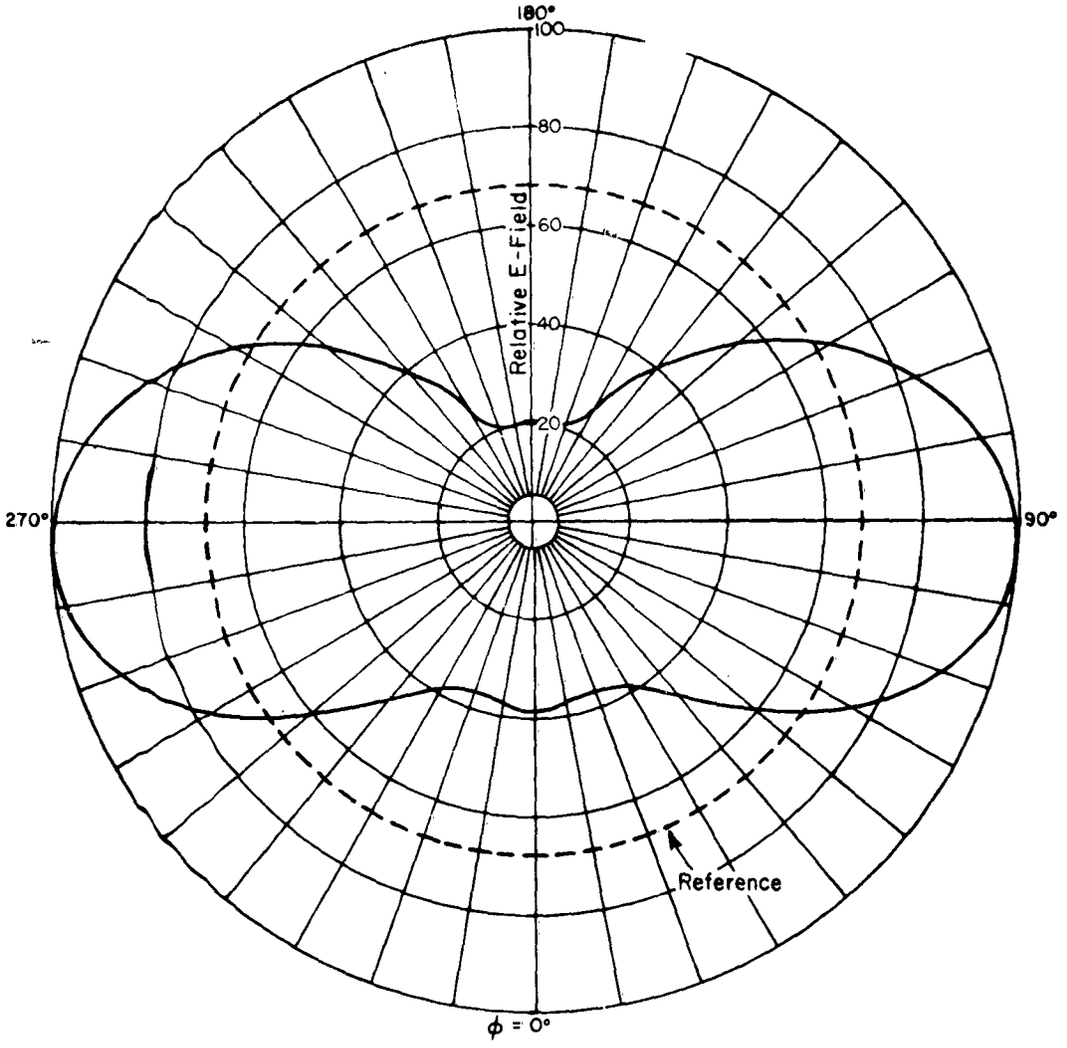

Fig. 12b. Theoretical far-field patterns of a circular cylinder.
(b) $d = \lambda/2$, $D = \lambda/2$.

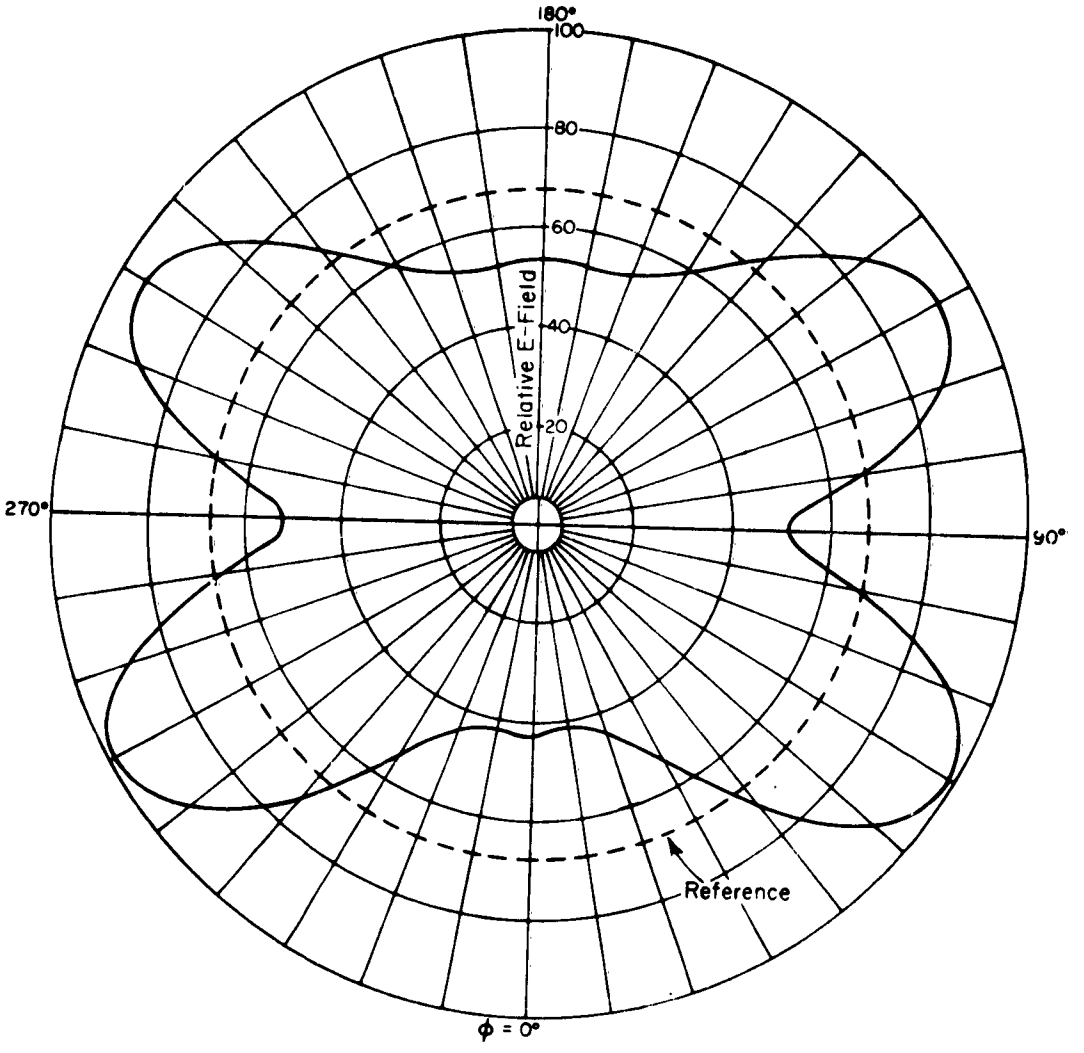

Fig. 12c. Theoretical far-field patterns of a circular cylinder.
(c) $d = \lambda$, $D = \lambda/4$.

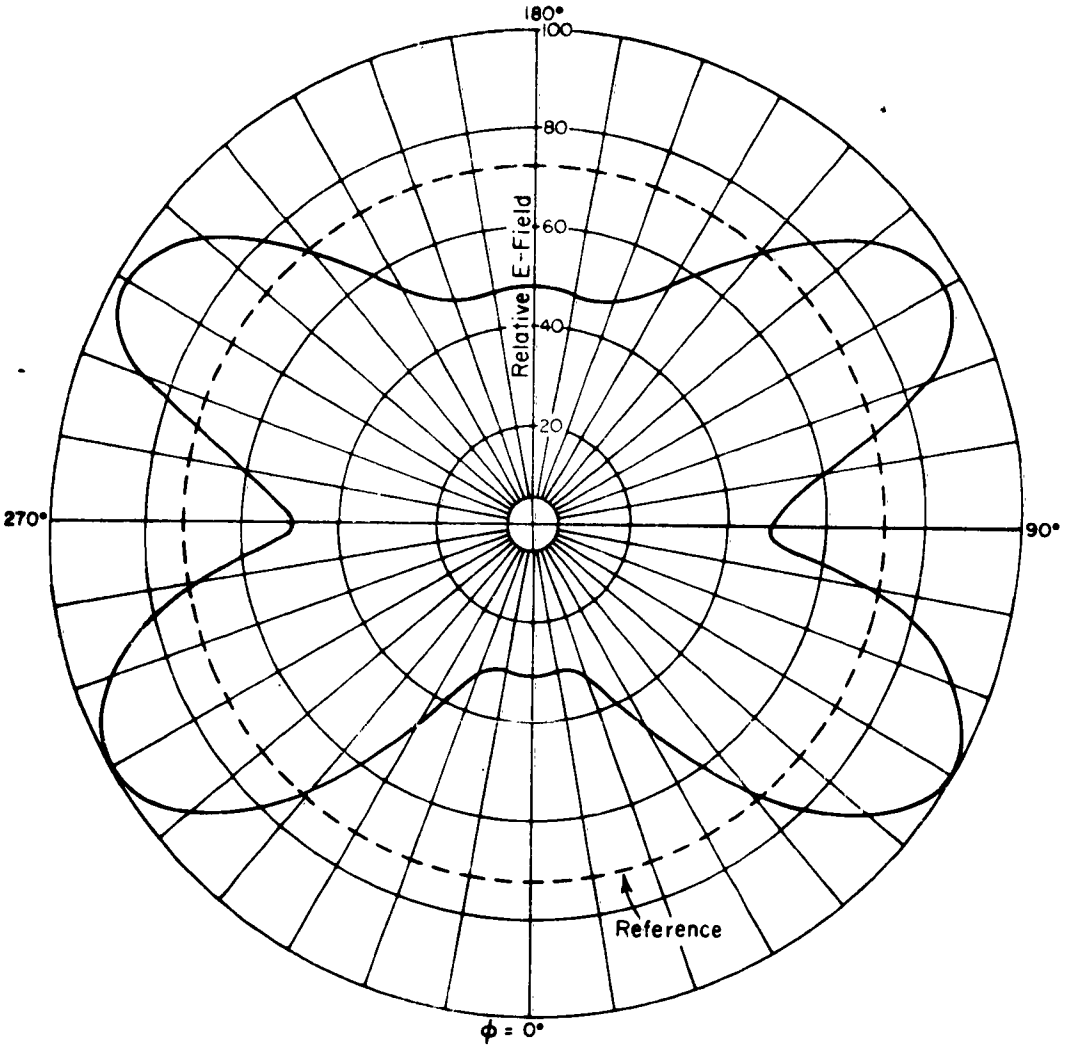

Fig. 12d. Theoretical far-field patterns of a circular cylinder.
(d) $d = \lambda$, $D = \lambda/2$.

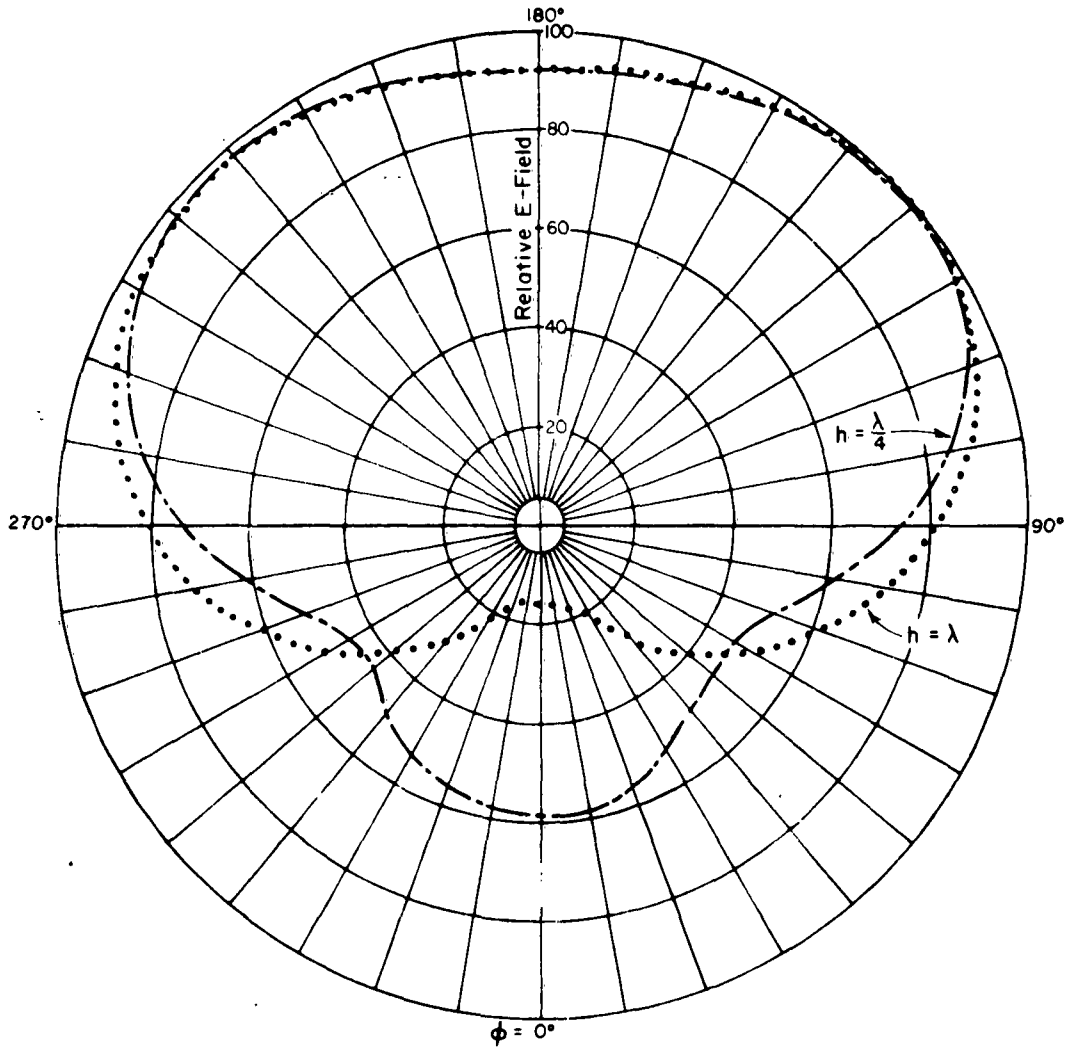

Fig. 13a. Effect of relative heights of source antenna and scatterer. Source antenna height = λ / 2.

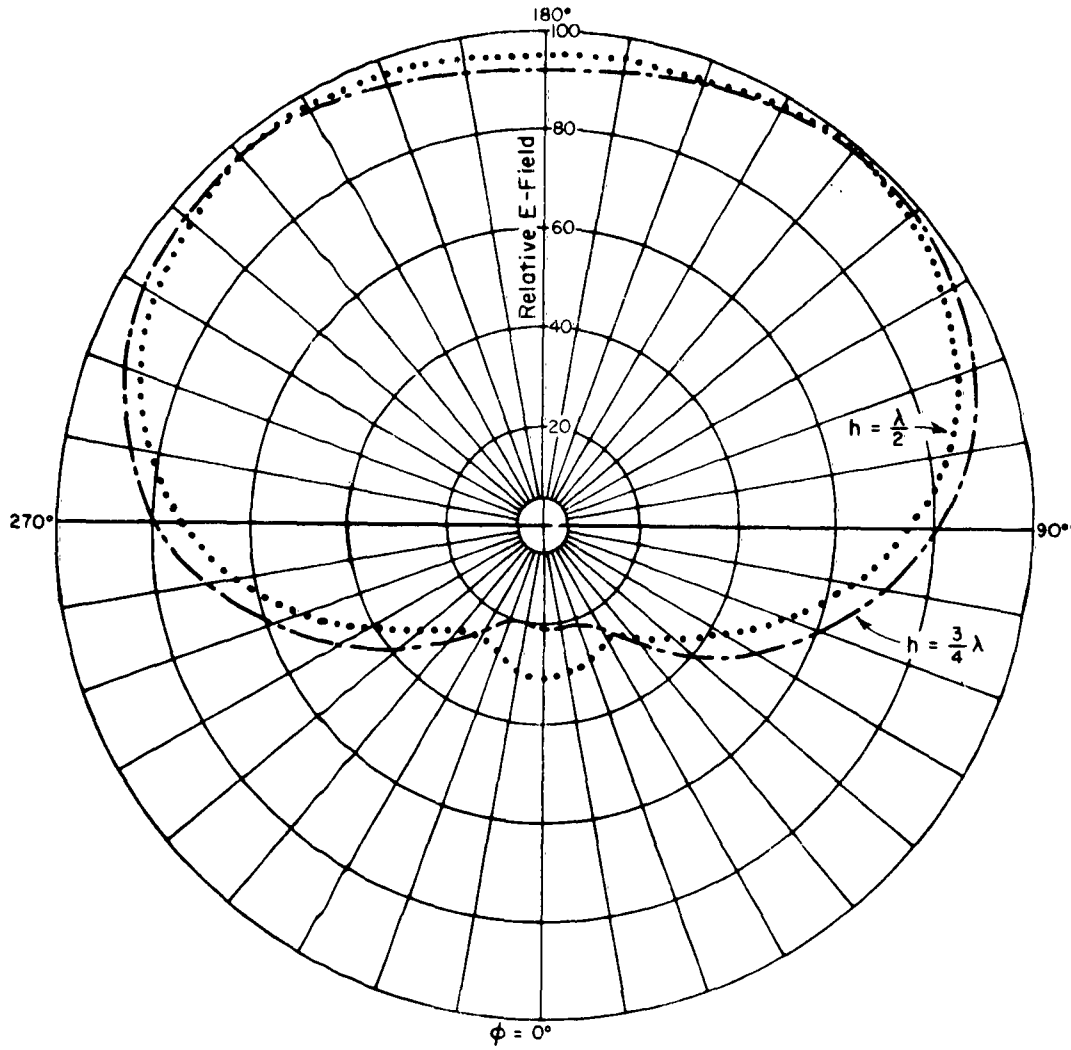

Fig. 13b. Effect of relative heights of source antenna and scatterer. Source antenna height = λ / 2.

storage is at a premium it is possible to omit those wires on the forward-scatter side where induced currents are relatively small and only slightly affect the far-field pattern.

This technique for far-field pattern prediction should find considerable use for the preliminary evaluation of shipboard situations where a vertical antenna of one or more elements has in its environment cylindrical scatterers with arbitrary cross-sections.

The program presented here indicates the practicality of the preparation of a handbook of patterns for a vertical antenna in the presence of scatterers of various sizes and shapes which would facilitate the optimum location of many shipboard antennas.

ACKNOWLEDGEMENT

The author wishes to express his appreciation to Dr. Jack H. Richmond for his help in devising the computer programs.

APPENDIX A
MATHEMATICAL DEVELOPMENT OF THE FORMULAS FOR THE FAR-FIELD PATTERNS

The problem of interest here is that of determining the far-field pattern in the horizontal plane due to a vertical antenna radiating near conducting cylinders of arbitrary cross-section. To obtain a mathematical model we approximate the conducting cylinder of arbitrary cross-section by an array of infinitely-long thin wires along the periphery and represent the vertical antenna by a vertical line source, as shown in Fig. 1.

The line source, whose current is directed in the positive z-direction, produces only a z-component of the electric field which is given by

$$E_z^i = -\frac{\omega\mu}{4} I H_o^{(2)}(k\rho) \tag{1}$$

where

$$k^2 = \omega^2 \mu \epsilon \tag{2}$$

and $H_o^{(2)}(k\rho)$ represents the zero-order Hankel function of the second kind. The current induced on wire n is uniform and produces a scattered field of the form

$$E_n^s = -\left(\frac{\omega\mu}{4}\right) I_n J_o(ka_n) H_o^{(2)}(k\rho_n) \tag{3}$$

for $\rho_n \geq a_n$,

where $J_o(ka_n)$ is the zero order Bessel function, a_n is the radius of wire n, and ρ_n is the distance from wire n. For convenience a "modified current" I_n' is defined by

$$I_n' = \left(\frac{\omega\mu}{4}\right) I_n J_o(ka_n). \tag{4}$$

Thus the field scattered from N wires at the surface of wire m can be written as

$$E_z^s = -\sum_{n=1}^{N} I_n' H_o^{(2)}(k\rho_{mn}) \tag{5}$$

where ρ_{mn} is the distance between wires m and n,

$$\rho_{mn} = \sqrt{(X_m - X_n)^2 + (Y_m - Y_n)^2} \quad , \tag{6}$$

and

$$\rho_{mm} = a_m \quad . \tag{7}$$

To obtain values for the complex current on each wire, we impose the condition that

$$E_z^i + E_z^s = 0 \tag{8}$$

at the surface of each wire. Actually we require that tangential E vanish at the center of each wire, which is an acceptable approximation for wires whose radii are much smaller than the wavelength. Substituting Eq.(1) and Eq.(5) with $\frac{\omega\mu}{4} I = -1$ into Eq.(8) we obtain

$$\sum_{n=1}^{N} H_o^{(2)}(k\rho_{mn})\, I_n' = H_o^{(2)}(k\rho_m) \quad . \tag{9}$$

The above equation then yields a set of N equations in the N unknowns I_n'. Having determined the complex currents on each wire, the far-field pattern can then be determined from

$$E_z(\phi) = +\sum_{n=1}^{N} H_o^{(2)}(k\rho_n)\, I_n' - H_o^{(2)}(k\rho) \quad . \tag{10}$$

When the observation point is at a great distance from the wires, it is said to be in the far-zone field. This permits some simplification of

Eq.(10). For large arguments the Hankel function can be approximated by the asymptotic formula

$$(11) \qquad H_o^{(2)}(X) \simeq \sqrt{2j/\pi X}\ e^{-jX}, \quad X \gg 1.$$

The distance from wire n at (X_n, Y_n) to the observation point at (ρ, ϕ) can be expressed as

$$(12) \qquad \rho_n \simeq \rho - X_n \cos\phi - Y_n \sin\phi \quad .$$

Consequently the far-field is given by

$$(13) \qquad E_z(\phi) = + \sqrt{\frac{2j}{\pi k \rho}}\ e^{-jk\rho} \left[-1 + \sum_{n=1}^{N} I_n'\, e^{jk(X_n \cos\phi + Y_n \sin\phi)} \right] .$$

A far-field pattern function is defined by the bracketed expression in Eq.(13), which can be written as

$$(14) \qquad F(\phi) = \sum_{n=o}^{N} I_n'\, e^{jk(X_n \cos\phi + Y_n \sin\phi)}$$

where $I_o' \equiv -1$ at the origin.

Appendix B gives three computer programs for implementing these calculations on a moderate-size (IBM-1620) computer. The first calculates the coefficients and excitation functions for the system of Eq.(9). The second solves the system for the modified currents I_n'. The last calculates the far field from these currents, according to Eq.(14). If only the scattered portion of the field is desired, the value of the current on the line source is set equal to zero in the input to this last program.

Appendix C gives a sample problem that illustrates the use of the three FORTRAN programs on the IBM 1620.

Appendix D gives a single, more efficient SCATRAN program for use on the IBM 7094 computer, which may be used in place of the three FORTRAN programs.

APPENDIX B

Figure 14 is a computer program in FORTRAN (Ohio State University Version 2) based on Eq.(9) for setting up the linear equations for the currents on the infinitely-long parallel wires. The line source is assumed to have a negative modified unit current. Included in the program is a subroutine for calculating the Bessel and Neumann functions. If the argument, $k\rho_{mn}$, is less than 4 the ascending power series is used and if it is greater than 4 the asymptotic series is used. The numbers in the "equals column" represent the incident electric field intensity at wire m due to the line source. Figure 15 gives a flow diagram for the program in Fig. 14. The output of the program in Fig. 14 is used as part of the input data for the program in Fig. 16. This program uses the method of Crout[2,3] to obtain the solution for an inhomogeneous system of linear equations with complex coefficients. The output of this program consists of the real and imaginary parts of the current on each wire.

Figure 17 gives a flow diagram for the program in Fig. 16. However, this program does not compute the elements in Crout's "auxiliary matrix" in the order called for by him in his article[2]. The order used here results in a more compact and efficient program.

The output of the program in Fig. 16, the various wire locations as used for input to the program of Fig. 14, and the magnitude of the line source current are used as the input for the program in Fig. 18. This latter program calculates the far-field pattern function of the parallel wire array excited by a line source whose "modified current" equals $-1 + j0$. If only the scattered field is desired, the input card for the magnitude of the line source current is omitted from the input deck. This program is based on Eq.(14). The output data gives the value of the pattern function at whatever values of ϕ are desired. Note that $E(\phi)$ in this program corresponds to the $F(\phi)$ defined by Eq.(14).

Figure 19 gives a flow diagram for the program in Fig. 18.

```
C     G THIELE, LINEAR EQUATIONS FOR SCATTERING PATTERN OF AN
C     ARBITRARY ARRAY OF THIN WIRES, LINE SOURCE AT THE ORIGIN
      DIMENSION U(56),V(56),F(29),G(29)
    2 FORMAT (F10.6,F10.6,F10.6,F10.6,F10.6,F10.6,F10.6,F10.6)
    3 FORMAT (I10,F10.6,F10.6,F10.6,F10.6,F10.6,F10.6,F10.6)
      READ 3,N,BKJ,BKY,AAA,THETA
  READ2,U(1),U(2),U(3),U(4),U(5),U(6),U(7),U(8)
  READ2,U(9),U(10),U(11),U(12),U(13),U(14),U(15),U(16)
      READ2,U(17),U(18),U(19),U(20),U(21),U(22),U(23)
  READ2,V(1),V(2),V(3),V(4),V(5),V(6),V(7),V(8)
  READ2,V(9),V(10),V(11),V(12),V(13),V(14),V(15),V(16)
      READ2,V(17),V(18),V(19),V(20),V(21),V(22),V(23)
       M = N
      NN = M+1
      THETA = .01745329*THETA
      STHET = SIN(THETA)
      IF(AAA)8,5,8
    5 STHET = 6.2831853*STHET
    8 DO 10 I = 1,M
      U(I) = STHET*U(I)
   10 V(I) = STHET*V(I)
      STHET = SIN(THETA)
   11 DO 15 I = 1,24
      F(I) = 0.
   15 G(I) = 0.
      DO 50 I = 1,M
      DO 17 K = 1,M
      F(K) = 0.
   17 G(K) = 0.
      DO 30 J = 1,N
      L = J
      IF(M-J)24,25,25
   24 L = J-M
   25 IF(I-J)14,12,14
   12 F(J) = BKJ
      G(J) =-BKY
      GO TO 30
   14 R=SQRT((U(I)-U(J))*(U(I)-U(J))+(V(I)-V(J))*(V(I)-V(J)))
      IJK = 1
      GO TO 34
   20 F(L) = F(L) + B
      G(L) = G(L)-Y
   30 CONTINUE
      R = SQRT(U(I)*U(I)+V(I)*V(I))
      IJK = 2
      GO TO 34
```

Symbols for Input Data

N	Number of wires
BKJ	$J_0(ka \sin \theta_o)$
BKY	$N_0^o(ka \sin \theta_o)$
AAA	0. if wire coordinates are x/λ and y/λ
	1. if wire coordinates are kx and ky
THETA	90.
U(N)	x coordinate of wire N
V(N)	y coordinate of wire N

Fig. 14. Digital computer program for setting up the linear equations for the N unknown currents.

```
45 F(NN) = B
   G(NN) = -Y
   PUNCH2,F(1),F(2),F(3),F(4),F(5),F(6),F(7),F(8)
   PUNCH2,F(9),F(10),F(11),F(12),F(13),F(14),F(15),F(16)
   PUNCH2,F(17),F(18),F(19),F(20),F(21),F(22),F(23),F(24)
   PUNCH2,G(1),G(2),G(3),G(4),G(5),G(6),G(7),G(8)
   PUNCH2,G(9),G(10),G(11),G(12),G(13),G(14),G(15),G(16)
50 PUNCH2,G(17),G(18),G(19),G(20),G(21),G(22),G(23),G(24)
   STOP
34 IF(R-4.)35,35,40
35 W = R/2.
    W1=W*W
    W2=W1*W1
    W3=W2*W1
    W4=W2*W2
    W5=W4*W1
    W6=W3*W3
    W7=W3*W4


    B=1.-W1+.25*W2-.027777*W3+.0017361*W4
    B=B-.6944E-4*W5+.1929E-5*W6-.394E-7*W7
    S=W1-.375*W2+.0509259*W3-.0036169*W4
    S=S+.15856E-3*W5-.4726E-5*W6+.1021E-6*W7
    Y=.63661977*(S+B*(.57721566+LOG(W)))
   GO TO 44
40 Z = 1./R
    X=Z*Z
    P=(1.-.07031*X+.11215*X*X)*.5641896
    Q=(.125-.07324*X)*Z*.5641896
    B=((P-Q)*COS(R)+(P+Q)*SIN(R))/SQRT(R)
    Y=((P-Q)*SIN(R)-(P+Q)*COS(R))/SQRT(R)
44 GO TO (20,45),IJK
   END
```

Fig. 14. Digital computer program for setting up the linear equations for the N unknown currents.

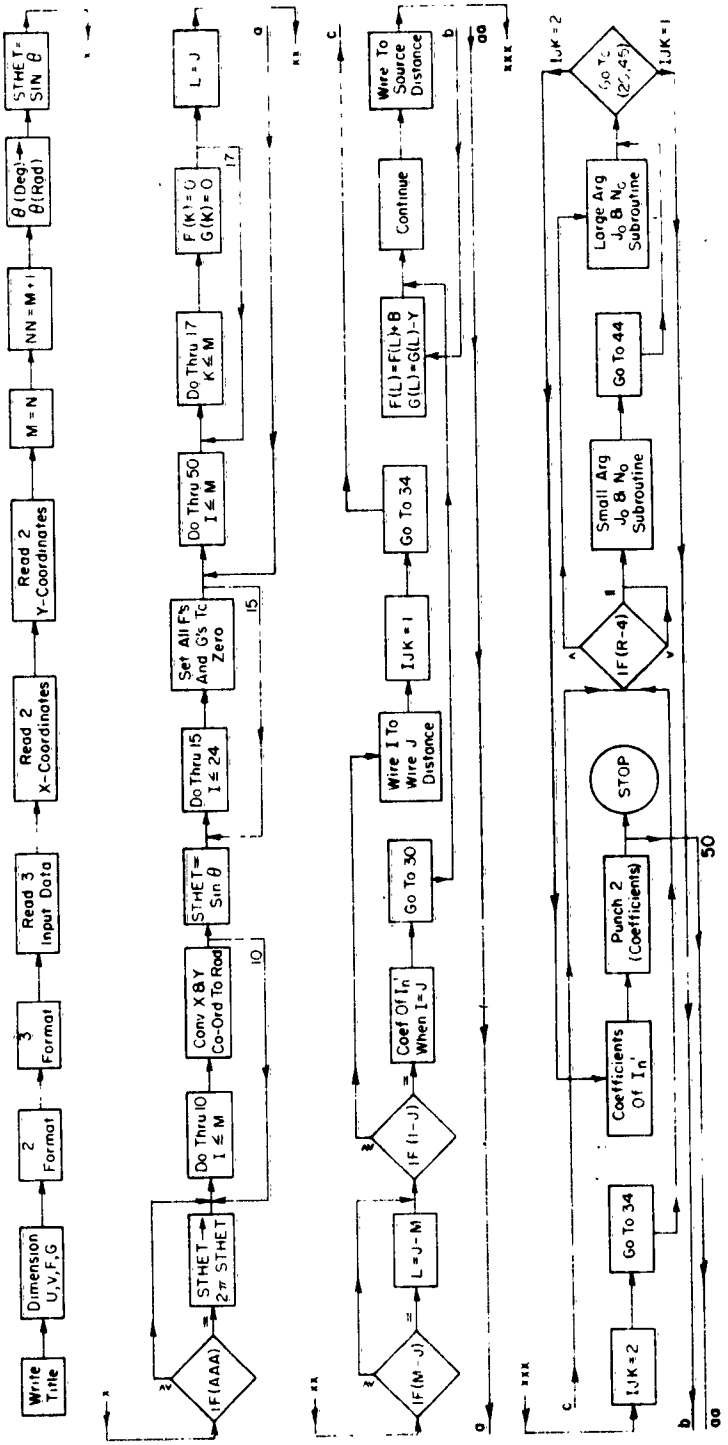

Fig. 15. Flow graph for the program in Fig. 14.

```
C       J RICHMOND, SOLUTION OF 15 (OR LESS) COMPLEX LINEAR EQUATIONS
        DIMENSION A(15,16),B(15,16)
 2      FORMAT (F10.6,F10.6,F10.6,F10.6,F10.6,F10.6,F10.6,F10.6)
 24     FORMAT (I5,F15.6,F15.6)
        READ I,N
        DO 5 I=1,N
   READ2,A(I,1),A(I,2),A(I,3),A(I,4),A(I,5),A(I,6),A(I,7),A(I,8)
   READ2,A(I,9),A(I,10),A(I,11),A(I,12),A(I,13),A(I,14),A(I,15),A(I,16)
   READ2,B(I,1),B(I,2),B(I,3),B(I,4),B(I,5),B(I,6),B(I,7),B(I,8)
 5 READ2,B(I,9),B(I,10),B(I,11),B(I,12),B(I,13),B(I,14),B(I,15),B(I,16)
        NN = N + 1
        DO 18 L = 1,N
        LLL = L-1
        DO 18 I = L,N
        II = I+1
        IF(LLL)5,4,3
 3      DO 17 K = 1,LLL
        A(I,L) = A(I,L) - A(I,K)*A(K,L) + B(I,K)*B(K,L)
        B(I,L) = B(I,L) - A(I,K)*B(K,L) - A(K,L)*B(I,K)
        A(L,II) = A(L,II) - A(L,K)*A(K,II) + B(L,K)*B(K,II)
 17     B(L,II) = B(L,II) - A(L,K)*B(K,II) - B(L,K)*A(K,II)
 4      R = A(L,L)*A(L,L) + B(L,L)*B(L,L)
        S= A(L,II)
        T = B(L,II)
        A(L,II) = (A(L,L)*S + B(L,L)*T)/R
 18     B(L,II) = (A(L,L)*T - B(L,L)*S)/R
        PUNCH 24,N,A(N,NN),B(N,NN)
        DO 23 L = 2,N
        I = NN-L
        II = I+1
        DO 22 K = II,N
        A(I,NN) = A(I,NN) - A(I,K)*A(K,NN) + B(I,K)*B(K,NN)
 22     B(I,NN) = B(I,NN) - A(I,K)*B(K,NN) - B(I,K)*A(K,NN)
 23     PUNCH 24,I,A(I,NN),B(I,NN)
        STOP
        END
```

Symbols for Input Data		Symbols for Output Data	
N	Number of Linear equations	I	Index of current I_i'
A(I,J)	Real part of coefficient of I_j' in equation i	A(I,NN)	Real part of current I_i'
B(I,J)	Imaginary part of coefficient of I_j' in equation i	B(I,NN)	Imaginary part of current I_i'

Fig. 16. Digital computer program for solving the system of of linear equations for the N unknown currents.

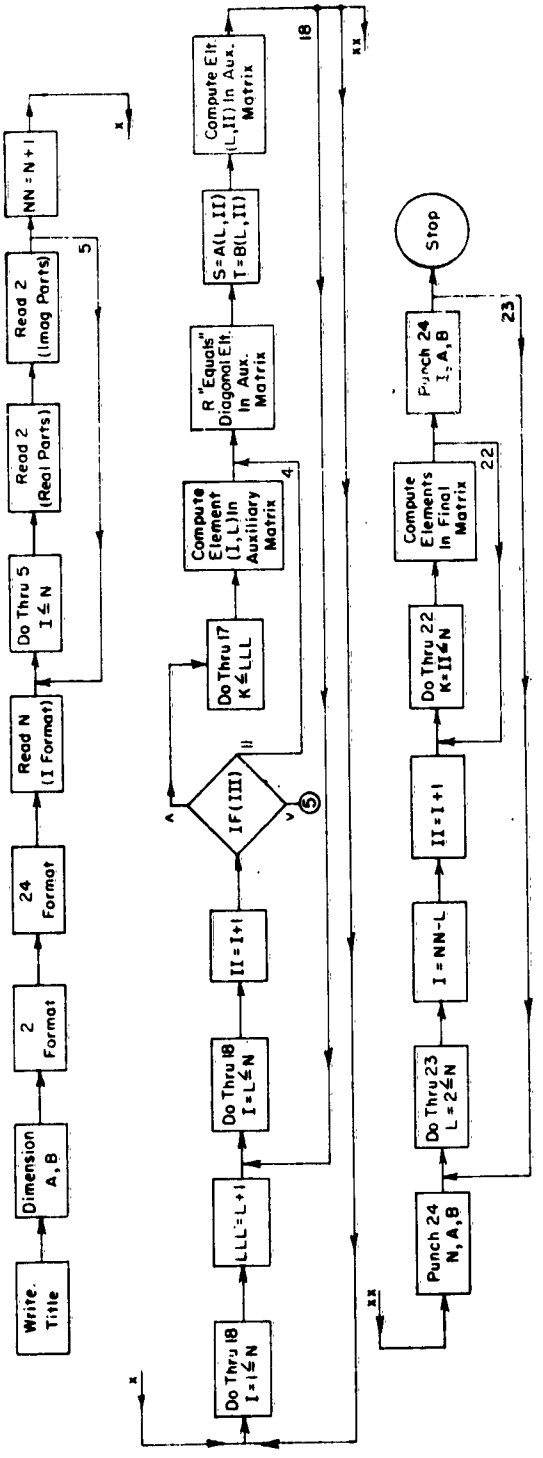

Fig. 17. Flow graph for the program in Fig. 16.

```
C   J RICHMOND, PATTERN OF ARRAY OF LINE SOURCES
      DIMENSION CR(30),CI(30),X(30),Y(30)
    2 FORMAT (I5,F15.8,F15.8,F15.8,F15.8,F15.8)
    3 FORMAT (F10.6,F10.6,F10.6,F10.6,F10.6,F10.6,F10.6,F10.6)
      READ 2,N,P,DP,FM,AAA,THETA
      READ 3,X(1),X(2),X(3),X(4),X(5),X(6),X(7),X(8)
      READ 3,X(9),X(10),X(11),X(12),X(13),X(14),X(15),X(16)
      READ3,X(17),X(18),X(19),X(20),X(21),X(22),X(23),X(24)
      READ 3,Y(1),Y(2),Y(3),Y(4),Y(5),Y(6),Y(7),Y(8)
      READ 3,Y(9),Y(10),Y(11),Y(12),Y(13),Y(14),Y(15),Y(16)
      READ3,Y(17),Y(18),Y(19),Y(20),Y(21),Y(22),Y(23),Y(24)
      THETA = .01745329*THETA
      STHET = SIN(THETA)
      IF(AAA)8,5,8
    5 STHET = 6.2831853*STHET
    8 DO 10 I = 1,N
      X(I) = STHET*X(I)
   10 Y(I) = STHET*Y(I)
   12 DO 20 I = 1,N
      READ 2,J,U,V
      CR(J) = U
      CI(J) = V
      CS = U*U + V*V
      CM = SQRT(CS)
   20 PUNCH 2,J,U,V,CS,CM
      M = FM
      DO 40 I = 1,M
      PR = .01745329*P
      C = COS(PR)
      S = SIN(PR)
      ER = 0.
      EI = 0.
      DO 30 J = 1,N
      Z = X(J)*C + Y(J)*S
      CZ = COS(Z)
      SZ = SIN(Z)
      ER = ER + CR(J)*CZ - CI(J)*SZ
   30 EI = EI + CI(J)*CZ + CR(J)*SZ
      ES = ER*ER + EI*EI
      E = SQRT(ES)
      PUNCH 2,I,P,ER,EI,ES,E
   40 P = P + DP
      STOP
      END
```

Symbols for Input Data

N	Number of wires
P	Initial value of ϕ in degrees
DP	Increment in ϕ in degrees
FM	Number of values of ϕ
AAA	0. if coordinates are x/λ and y/λ 1. if coordinates are kx and ky
THETA	Angle of incidence θ_o with respect to z axis
X(N)	x/λ or kx (coordinate of wire n)
Y(N)	y/λ or ky (coordinate of wire n)
J	Index number of wire j
U	Real part of current on wire j
V	Imaginary current on wire j

Symbols for Output Data

P	Angle ϕ in degrees
ER	Real part of $E(\phi)$
EI	Imaginary part of $E(\phi)$
ES	Magnitude squared of $E(\phi)$
E	Magnitude of $E(\phi)$

Fig. 18. Digital computer program for the far-field pattern of an arbitrary array of parallel wires.

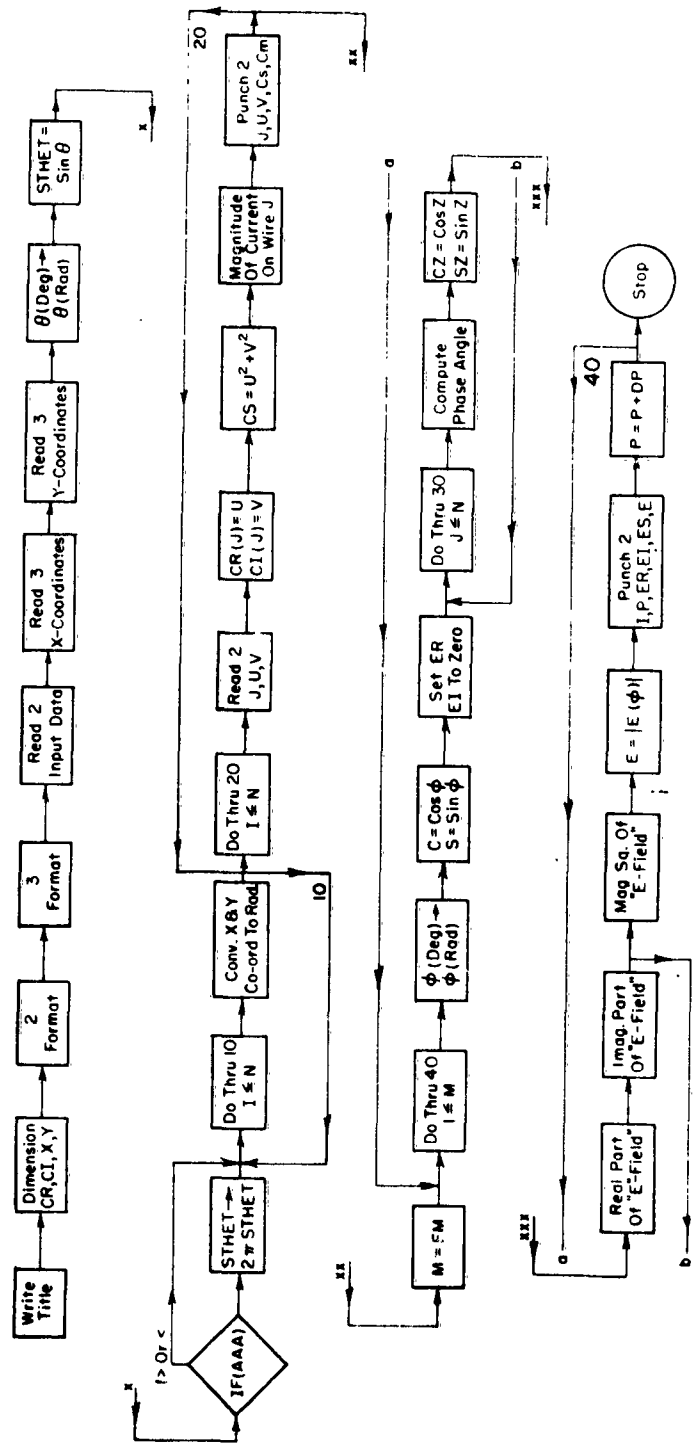

Fig. 19. Flow graph for the program in Fig. 18.

APPENDIX C

The purpose of this appendix is to minimize the time required to gain proficiency in the utilization of the programs in Appendix B. As a sample calculation, the situation in Fig. 4 was used with $d = \lambda/2$ and $\ell = \lambda/4$. Three wires were used on a side as opposed to the five that were used to obtain the theoretical pattern in Fig. 5b.

The input cards to the program of Fig. 14 are shown in Fig. 20 and are self-explanatory except possibly for the four "zero" cards which are necessary because the program can accommodate up to 24 wires and only 8 are used in this instance. The output from this program consists of the real and imaginary parts of the coefficients of I_n'. Again, since the program provides for up to 24 wires but only 8 are used in this example, some of the output cards contain only zeros. These "zero cards" are removed before using the output as the input for the program of Fig. 16. The output of that computation is just the real and imaginary parts of the currents on each of the 8 wires. These cards are then used as part of the input to the program of Fig.18. Note that the same coordinate information used for Fig. 14 is also used for Fig. 18. Also note that the "current" $-1 + j0$ of the line source must be included in the input unless just the scattered field is desired. The output of the Fig. 18 program contains the desired far-field pattern information in the right-most column. These numbers may be used to generate the normalized pattern in Fig. 5b which was calculated using 5 wires per side and therefore has slightly deeper nulls. If in this example the only wire were the line source itself, the output of the last program (Fig. 18) would indicate that $F(\phi) = 1$. Hence the unit circle may be used as a reference.

```
C     INPUT CARDS FOR PROGRAM IN FIG 14
          8      .99937    -1.97931       0.0        90.0
      0.500       0.500       0.625       0.750       0.750       0.750       0.625       0.500
        0.0
        0.0
      0.000       0.125       0.125       0.125       0.000      -0.125      -0.125      -0.125
        0.0
        0.0

C     OUTPUT CARDS FROM PROGRAM IN FIG 14
  +.999370  +.851631  +.714556  +.365432  +.472001  +.365432  +.714556  +.851631
  -.304243  +.000000  +.000000  +.000000  +.000000  +.000000  +.000000  +.000000
  +.000000  +.000000  +.000000  +.000000  +.000000  +.000000  +.000000  +.000000
 +1.979310  +.101207  -.169601  -.467056  -.410003  -.467056  -.169601  +.101207
  -.328366  +.000000  +.000000  +.000000  +.000000  +.000000  +.000000  +.000000
  +.000000  +.000000  +.000000  +.000000  +.000000  +.000000  +.000000  +.000000
  +.851631  +.999370  +.851631  +.472001  +.365432  +.098474  +.365432  +.472001
  -.329898  +.000000  +.000000  +.000000  +.000000  +.000000  +.000000  +.000000
  +.000000  +.000000  +.000000  +.000000  +.000000  +.000000  +.000000  +.000000
  +.101207 +1.979310  +.101207  -.410003  -.467056  -.520633  -.467056  -.410003
  -.292726  +.000000  +.000000  +.000000  +.000000  +.000000  +.000000  +.000000
  +.000000  +.000000  +.000000  +.000000  +.000000  +.000000  +.000000  +.000000
  +.714556  +.851631  +.999370  +.851631  +.714556  +.365432  +.472001  +.365432
  -.396862  +.000000  +.000000  +.000000  +.000000  +.000000  +.000000  +.000000
  +.000000  +.000000  +.000000  +.000000  +.000000  +.000000  +.000000  +.000000
  -.169601  +.101207 +1.979310  +.101207  -.169601  -.467056  -.410003  -.467056
  +.018899  +.000000  +.000000  +.000000  +.000000  +.000000  +.000000  +.000000
  +.000000  +.000000  +.000000  +.000000  +.000000  +.000000  +.000000  +.000000
  +.365432  +.472001  +.851631  +.999370  +.851631  +.472001  +.365432  +.098474
  -.247116  +.000000  +.000000  +.000000  +.000000  +.000000  +.000000  +.000000
  +.000000  +.000000  +.000000  +.000000  +.000000  +.000000  +.000000  +.000000
  -.467056  -.410003  +.101207 +1.979310  +.101207  -.410003  -.467056  -.520633
  +.267421  +.000000  +.000000  +.000000  +.000000  +.000000  +.000000  +.000000
  +.000000  +.000000  +.000000  +.000000  +.000000  +.000000  +.000000  +.000000
  +.472001  +.365432  +.714556  +.851631  +.999370  +.851631  +.714556  +.365432
  -.265847  +.000000  +.000000  +.000000  +.000000  +.000000  +.000000  +.000000
  +.000000  +.000000  +.000000  +.000000  +.000000  +.000000  +.000000  +.000000
  -.410003  -.467056  -.169601  +.101207 +1.979310  +.101207  -.169601  -.467056
  +.252423  +.000000  +.000000  +.000000  +.000000  +.000000  +.000000  +.000000
  +.000000  +.000000  +.000000  +.000000  +.000000  +.000000  +.000000  +.000000
  +.365432  +.098474  +.365432  +.472001  +.851631  +.999370  +.851631  +.472001
  -.247116  +.000000  +.000000  +.000000  +.000000  +.000000  +.000000  +.000000
  +.000000  +.000000  +.000000  +.000000  +.000000  +.000000  +.000000  +.000000
  -.467056  -.520633  -.467056  -.410003  +.101207 +1.979310  +.101207  -.410003
  +.267421  +.000000  +.000000  +.000000  +.000000  +.000000  +.000000  +.000000
  +.000000  +.000000  +.000000  +.000000  +.000000  +.000000  +.000000  +.000000
  +.714556  +.365432  +.472001  +.365432  +.714556  +.851631  +.999370  +.851631
  -.396862  +.000000  +.000000  +.000000  +.000000  +.000000  +.000000  +.000000
  +.000000  +.000000  +.000000  +.000000  +.000000  +.000000  +.000000  +.000000
  -.169601  -.467056  -.410003  -.467056  -.169601  +.101207 +1.979310  +.101207
  +.018899  +.000000  +.000000  +.000000  +.000000  +.000000  +.000000  +.000000
  +.000000  +.000000  +.000000  +.000000  +.000000  +.000000  +.000000  +.000000
  +.851631  +.472001  +.365432  +.098474  +.365432  +.472001  +.851631  +.999370
  -.329898  +.000000  +.000000  +.000000  +.000000  +.000000  +.000000  +.000000
  +.000000  +.000000  +.000000  +.000000  +.000000  +.000000  +.000000  +.000000
  +.101207  -.410003  -.467056  -.520633  -.467056  -.410003  +.101207 +1.979310
  -.292726  +.000000  +.000000  +.000000  +.000000  +.000000  +.000000  +.000000
  +.000000  +.000000  +.000000  +.000000  +.000000  +.000000  +.000000  +.000000
```

Fig. 20. Inputs and outputs of the programs in appendices A, B, and C.

```
C     INPUT CARDS FOR PROGRAM IN FIG 16
         8
   +.999370   +.851631   +.714556   +.365432   +.472001   +.365432   +.714556   +.851631
   -.304243   +.000000   +.000000   +.000000   +.000000   +.000000   +.000000   +.000000
  +1.979310   +.101207   -.169601   -.467056   -.410003   -.467056   -.169601   +.101207
   -.328366   +.000000   +.000000   +.000000   +.000000   +.000000   +.000000   +.000000
   +.851631   +.999370   +.851631   +.472001   +.365432   +.098474   +.365432   +.472001
   -.329898   +.000000   +.000000   +.000000   +.000000   +.000000   +.000000   +.000000
   +.101207  +1.979310   +.101207   -.410003   -.467056   -.520633   -.467056   -.410003
   -.292726   +.000000   +.000000   +.000000   +.000000   +.000000   +.000000   +.000000
   +.714556   +.851631   +.999370   +.851631   +.714556   +.365432   +.472001   +.365432
   -.396862   +.000000   +.000000   +.000000   +.000000   +.000000   +.000000   +.000000
   -.169601   +.101207  +1.979310   +.101207   -.169601   -.467056   -.410003   -.467056
   +.018899   +.000000   +.000000   +.000000   +.000000   +.000000   +.000000   +.000000
   +.365432   +.472001   +.851631   +.999370   +.851631   +.472001   +.365432   +.098474
   -.247116   +.000000   +.000000   +.000000   +.000000   +.000000   +.000000   +.000000
   -.467056   -.410003   +.101207  +1.979310   +.101207   -.410003   -.467056   -.520633
   +.267421   +.000000   +.000000   +.000000   +.000000   +.000000   +.000000   +.000000
   +.472001   +.365432   +.714556   +.851631   +.999370   +.851631   +.714556   +.365432
   -.265847   +.000000   +.000000   +.000000   +.000000   +.000000   +.000000   +.000000
   -.410003   -.467056   -.169601   +.101207  +1.979310   +.101207   -.169601   -.467056
   +.252423   +.000000   +.000000   +.000000   +.000000   +.000000   +.000000   +.000000
   +.365432   +.098474   +.365432   +.472001   +.851631   +.999370   +.851631   +.472001
   -.247116   +.000000   +.000000   +.000000   +.000000   +.000000   +.000000   +.000000
   -.467056   -.520633   -.467056   -.410003   +.101207  +1.979310   +.101207   -.410003
   +.267421   +.000000   +.000000   +.000000   +.000000   +.000000   +.000000   +.000000
   +.714556   +.365432   +.472001   +.365432   +.714556   +.851631   +.999370   +.851631
   -.396862   +.000000   +.000000   +.000000   +.000000   +.000000   +.000000   +.000000
   -.169601   -.467056   -.410003   -.467056   -.169601   +.101207  +1.979310   +.101207
   +.018899   +.000000   +.000000   +.000000   +.000000   +.000000   +.000000   +.000000
   +.851631   +.472001   +.365432   +.098474   +.365432   +.472001   +.851631   +.999370
   -.329898   +.000000   +.000000   +.000000   +.000000   +.000000   +.000000   +.000000
   +.101207   -.410003   -.467056   -.520633   -.467056   -.410003   +.101207  +1.979310
   -.292726   +.000000   +.000000   +.000000   +.000000   +.000000   +.000000   +.000000

C     OUTPUT CARDS FROM PROGRAM IN FIG 16
   +8        -.161631        -.018926
   +7        -.038466        +.028586
   +6        +.005762        +.019949
   +5        -.000098        +.000905
   +4        +.005762        +.019949
   +3        -.038466        +.028586
   +2        -.161631        -.018926
   +1        -.133808        -.062170

C     INPUT CARDS FOR PROGRAM IN FIG 18
    9              0.0              10.0              36.0              0.0              90.0

    0.500     0.500     0.625     0.750     0.750     0.750     0.625     0.500
      0.0
      0.0
    0.000     0.125     0.125     0.125     0.000    -0.125    -0.125    -0.125
      0.0
      0.0
    9              -1.0              0.0
   +8        -.161631        -.018926
   +7        -.038466        +.028586
   +6        +.005762        +.019949
   +5        -.000098        +.000905
   +4        +.005762        +.019949
   +3        -.038466        +.028586
   +2        -.161631        -.018926
   +1        -.133808        -.062170
```

Fig. 20. Inputs and outputs of the programs in appendices A, B, and C.

```
C     OUTPUT CARDS FROM PROGRAM IN FIG 18
  +9     -1.00000000      +.00000000     +1.00000000     +1.00000000
  +8      -.16163100      -.01892600      +.02648277      +.16273528
  +7      -.03846600      +.02858600      +.00229679      +.04792486
  +6      +.00576200      +.01994900      +.00043116      +.02076447
  +5      -.00009800      +.00009500      +.00000082      +.00091029
  +4      +.00576200      +.01994900      +.00043116      +.02076447
  +3      -.03846600      +.02858600      +.00229679      +.04792486
  +2      -.16163100      -.01892600      +.02648277      +.16273528
  +1      -.13380800      -.06217000      +.02176969      +.14754555
  +1      +.00000000      -.40730116      +.10256843      +.17641451      +.42001727
  +2    +10.00000000      -.40757072      +.07192805      +.17128753      +.41386897
  +3    +20.00000000      -.41717391      -.01696248      +.17432180      +.41751862
  +4    +30.00000000      -.45908866      -.15166895      +.23376587      +.48349340
  +5    +40.00000000      -.55959657      -.30378805      +.40543550      +.63673817
  +6    +50.00000000      -.73096286      -.42788042      +.71738835      +.84698780
  +7    +60.00000000      -.95541772      -.47370881     +1.13722310     +1.06640660
  +8    +70.00000000     -1.18309290      -.40961800     +1.56749570     +1.25199660
  +9    +80.00000000     -1.35024300      -.24259704     +1.88200950     +1.37185350
 +10    +90.00000000     -1.40873720      -.01939185     +1.98491650     +1.40887060
 +11   +100.00000000     -1.34830170      +.19377559     +1.85546650     +1.36215500
 +12   +110.00000000     -1.19848000      +.34034474     +1.55218880     +1.24586860
 +13   +120.00000000     -1.01133640      +.39454128     +1.17846410     +1.08557080
 +14   +130.00000000      -.83707761      +.36484096      +.83380786      +.91313080
 +15   +140.00000000      -.70644604      +.28205393      +.57862043      +.76067103
 +16   +150.00000000      -.62652430      +.18230454      +.42576765      +.65250873
 +17   +160.00000000      -.58741117      +.09461487      +.35400386      +.59498223
 +18   +170.00000000      -.57292317      +.03666559      +.32958533      +.57409522
 +19   +180.00000000      -.56976057      +.01662214      +.32490341      +.57000299
 +20   +190.00000000      -.57292313      +.03666538      +.32958526      +.57409516
 +21   +200.00000000      -.58741106      +.09461452      +.35400366      +.59498206
 +22   +210.00000000      -.62652402      +.18230404      +.42576711      +.65250832
 +23   +220.00000000      -.70644550      +.28205340      +.57861936      +.76067033
 +24   +230.00000000      -.83707676      +.36484062      +.83380618      +.91312988
 +25   +240.00000000     -1.01133550      +.39454130     +1.17846230     +1.08557000
 +26   +250.00000000     -1.19847910      +.34034526     +1.55218710     +1.24586800
 +27   +260.00000000     -1.34830110      +.19377658     +1.85546530     +1.36215460
 +28   +270.00000000     -1.40873720      -.01939065     +1.98491650     +1.40887060
 +29   +280.00000000     -1.35024360      -.24259598     +1.88201060     +1.37186390
 +30   +290.00000000     -1.18309400      -.40961738     +1.56749780     +1.25199750
 +31   +300.00000000      -.95541896      -.47370878     +1.13722540     +1.06640770
 +32   +310.00000000      -.73096395      -.42788091      +.71739037      +.84698900
 +33   +320.00000000      -.55959727      -.30378879      +.40543673      +.63673913
 +34   +330.00000000      -.45908900      -.15166970      +.23376641      +.48349396
 +35   +340.00000000      -.41717405      -.01696307      +.17432194      +.41751878
 +36   +350.00000000      -.40757074      +.07192772      +.17128751      +.41386895
```

Fig. 20. Inputs and outputs of the programs in appendices A, B, and C.

APPENDIX D

Figure 21 is a SCATRAN[4] program for use on the IBM 7090 computer at the Ohio State University. By combining the programs in Appendix B into a single SCATRAN program and utilizing the greater speed of the IBM 7090, this program achieves the same results in about 1/50 th the time it takes the IBM 1620. In addition, the IBM 7090 provides more storage capacity which is necessary for the solution of arrays with large numbers of wires.

```
 THIELE, G.                    JOBN FGJ176                                    01/13/65
   SA          WRITE OUTPUT ,S1-                                                0028
 F S1         (///78H SCATTERING BY ARBITRARY ARRAY OF THIN WIRES WITH A        0029
              LINE SOURCE AT THE ORIGIN///) -                                  0030
               IJK=62-                                                         0031
               DIMENSION (U(61),V(61))-                                        0032
               DIMENSION (A(3782,IJK),B(3782,IJK))-                            0033
 F S2         (7F10.6)     -                                                   0034
               READ INPUT ,S5,(III)-                                          0035
               DO THROUGH (S260),JJJ=1,1,JJJ.LE.III-                          0036
               READ INPUT ,S2,(FN,BKJ,BKY,AAA,PHI)-                           0037
              N=FN-                                                           0038
               READ INPUT ,S2,((U(I),I=1,1,I.LE.N))-                          0039
               READ INPUT ,S2,((V(I),I=1,1,I.LE.N))-                          0040
               DO THROUGH (S4),I=1,1,I.LE.N-                                  0041
              U(I)=6.2831853*U(I)-                                            0042
   S4         V(I)=6.2831853*V(I)-                                            0043
              NN=N+1-                                                         0044
               WRITE OUTPUT ,S10-                                             0045
 F S5         (2I5,F15.8) -                                                   0046
 F S10        (///27H INTERWIRE SPACING KR(I,J)///)     -                     0047
               DO THROUGH (S50),I=1,1,I.LE.N-                                 0048
               DO THROUGH (S30),J=1,1,J.LE.N-                                 0049
               TRANSFER TO (S14,S12,S14) PROVIDED (I-J)-                      0050
   S12        A(I,J)=BKJ-                                                     0051
              B(I,J)=-BKY-                                                    0052
               TRANSFER TO (S30)-                                             0053
   S14        R=SQRT.((U(I)-U(J))*(U(I)-U(J))+(V(I)-V(J))*(V(I)-V(J)))-       0054
               WRITE OUTPUT ,S5,(I,J,R)-                                      0055
               TRANSFER TO (S16,S16,S18) PROVIDED (R-4.)-                     0056
   S16        W=R/2.-                                                         0057
              W1=W*W-                                                         0058
              W2=W1*W1-                                                       0059
              W3=W2*W1-                                                       0060
              W4=W2*W2-                                                       0061
              W5=W4*W1-                                                       0062
              W6=W3*W3-                                                       0063
              W7=W3*W4-                                                       0064
              BB=1.-W1+.25*W2-.0277778*W3+.0017361*W4-                        0065
              BB=BB-.6944.X.-4*W5+.1929.X.-5*W6-.394.X.-7*W7-                 0066
              S=W1-.375*W2+.0509259*W3-.0036169*W4-                           0067
              S=S+.15856.X.-3*W5-.4726.X.-5*W6+.1021.X.-6*W7-                 0068
              Y=.63661977*(S+BB*(.57721566+LN.(W)))-                          0069
               TRANSFER TO (S20)-                                             0070
```

Fig. 21. SCATRAN program for obtaining the far-field pattern of an arbitrary array with a line source at the origin.

```
S18         Z=1.0/R-                                                        0071
            X=Z*Z-                                                          0072
            P=(1.0-.07031*X+.11215*X*X)*.5641896-                           0073
            Q=(.125-.07324*X)*Z*.5641896-                                   0074
            BB=((P-Q)*COS.(R)+(P+Q)*SIN.(R))/SQRT.(R)-                      0075
            Y=((P-Q)*SIN.(R)-(P+Q)*COS.(R))/SQRT.(R)-                       0076
S20         A(I,J)=BB-                                                      0077
            B(I,J)=-Y-                                                      0078
S30          CONTINUE -                                                     0079
            R=SQRT.(U(I)*U(I)+V(I)*V(I))-                                   0080
             TRANSFER TO (S36,S36,S38) PROVIDED (R-4.)-                     0081
S36         W=R/2.0-                                                        0082
            W1=W*W-                                                         0083
            W2=W1*W1-                                                       0084
            W3=W2*W1-                                                       0085
            W4=W2*W2-                                                       0086
            W5=W4*W1-                                                       0087
            W6=W3*W3-                                                       0088
            W7=W3*W4-                                                       0089
            BB=1.-W1+.25*W2-.0277778*W3+.0017361*W4-                        0090
            BB=BB-.6944.X.-4*W5+.1929.X.-5*W6-.394.X.-7*W7-                 0091
            S=W1-.375*W2+.0509259*W3-.0036169*W4-                           0092
            S=S+.15856.X.-3*W5-.4726.X.-5*W6+.1021.X.-6*W7-                 0093
            Y=.03661977*(S+BB*(.57721566+LN.(W)))-                          0094
             TRANSFER TO (S49)-                                             0095
S38         Z=1.0/R-                                                        0096
            X=Z*Z-                                                          0097
            P=(1.0-.07031*X+.11215*X*X)*.5641896-                           0098
            Q=(.125-.07324*X)*Z*.5641896-                                   0099
            BB=((P-Q)*COS.(R)+(P+Q)*SIN.(R))/SQRT.(R)-                      0100
            Y=((P-Q)*SIN.(R)-(P+Q)*COS.(R))/SQRT.(R)-                       0101
S49         B(I,NN)=-Y-                                                     0102
S50         A(I,NN)=BB-                                                     0103
             WRITE OUTPUT ,S2,(((A(I,J),J=1,1,J.LE.NN),I=1,1,I.LE.N))-      0104
             WRITE OUTPUT ,S2,(((B(I,J),J=1,1,J.LE.NN),I=1,1,I.LE.N))-      0105
             WRITE OUTPUT ,S60-                                             0106
F S60       (///46H REAL AND IMAGINARY PARTS OF CURRENT ON WIRE I///)        0107
            -                                                               0108
F S80       (15,2F15.8) -                                                   0109
             DO THROUGH (S118),L=1,1,L.LE.N-                                0110
            LLL = L - 1 -                                                   0111
             DO THROUGH (S118),I=L,1,I.LE.N-                                0112
            II=I+1-                                                         0113
             TRANSFER TO (S104,S104,S103) PROVIDED (LLL)-                   0114
```

Fig. 21. SCATRAN program for obtaining the far-field pattern of an arbitrary array with a line source at the origin.

```
      S103        DO THROUGH (S117),K=1,1,K.LE.LLL-                          0115
                  A(I,L)=A(I,L)-A(I,K)*A(K,L)+B(I,K)*B(K,L)-                 0116
                  B(I,L)=B(I,L)-A(I,K)*B(K,L)-A(K,L)*B(I,K)-                 0117
                  A(L,II)=A(L,II)-A(L,K)*A(K,II)+B(L,K)*B(K,II)-             0118
      S117        B(L,II)=B(L,II)-A(L,K)*B(K,II)-B(L,K)*A(K,II)-             0119
      S104        R=A(L,L)*A(L,L)+B(L,L)*B(L,L)-                             0120
                  S=A(L,II)-                                                 0121
                  T=B(L,II)-                                                 0122
                  A(L,II)=(A(L,L)*S+B(L,L)*T)/R-                             0123
      S118        B(L,II)=(A(L,L)*T-B(L,L)*S)/R-                             0124
                   WRITE OUTPUT ,S80,(N,A(N,NN),B(N,NN))-                    0125
                   DO THROUGH (S123),L=2,1,L.LE.N-                           0126
                  I=NN-L-                                                    0127
                  II=I+1-                                                    0128
                   DO THROUGH (S122),K=II,1,K.LE.N-                          0129
                  A(I,NN)=A(I,NN)-A(I,K)*A(K,NN)+B(I,K)*B(K,NN)-             0130
      S122        B(I,NN)=B(I,NN)-A(I,K)*B(K,NN)-B(I,K)*A(K,NN)-             0131
      S123         WRITE OUTPUT ,S80,(I,A(I,NN),B(I,NN))-                    0132
                   WRITE OUTPUT ,S200-                                       0133
    F S200        (///18H FAR FIELD PATTERN///) -                            0134
                   READ INPUT ,S2,(P,DP,FM)-                                0135
                  M=FM-                                                      0136
                  A(0,NN)=-1-                                                0137
                  B(0,NN)=.0-                                                0138
                  U(0)=.0-                                                   0139
                  V(0)=.0-                                                   0140
                   DO THROUGH (S240),I=1,1,I.LE.M-                           0141
                  PR=.01745329*P-                                            0142
                  C=COS.(PR)-                                                0143
                  S=SIN.(PR)-                                                0144
                  ER=0.-                                                     0145
                  EI=0.-                                                     0146
                   DO THROUGH (S230),J=0,1,J.LE.N-                           0147
                  Z=U(J)*C+V(J)*S-                                           0148
                  CZ=COS.(Z)-                                                0149
                  SZ=SIN.(Z)-                                                0150
                  ER=ER+A(J,NN)*CZ-B(J,NN)*SZ-                               0151
      S230        EI=EI+B(J,NN)*CZ+A(J,NN)*SZ-                               0152
                  ES=ER*ER+EI*EI-                                            0153
                  E=SQRT.(ES)-                                               0154


                   WRITE OUTPUT ,S250,(P,ER,EI,ES,E)-                        0155
      S240        P=P+DP-                                                    0156
    F S250        (5F14.8)     -                                             0157
      S260         WRITE OUTPUT ,S1-                                        0158
                   END PROGRAM (SA)-                                        0159
```

Fig. 21. SCATRAN program for obtaining the far-field pattern of an arbitrary array with a line source at the origin.

REFERENCES

1. Richmond, Jack H., "Scattering by an Arbitrary Array of Parallel Wires", Report 1522-7, 30 April 1964, Antenna Laboratory, The Ohio State University Research Foundation; prepared under contract N 123 (953)-31663A, United States Navy Electronics Laboratory, San Diego, California (AD443 833).

2. Crout, P.D., "A Short Method for Evaluating Determinants and Solving Systems of Linear Equations with Real or Complex Coefficients", AIEE Transactions, Vol. 60, 1941, pp. 1235-1241.

3. Introduction to Numerical Analysis by Hildebrand, pp 429-434, McGraw Hill Book Company, 1956.

4. "Scatran Reference Manual", Copyright 1964 by The Numerical Computation Laboratory, The Ohio State University.